이학박사학위청구논문

지방세포 형태 변화에 의한 인슐린 의존적 포도당 흡수능 조절 기전 연구

Roles of adipocyte lipid droplets in the regulation of insulin-dependent glucose uptake

2019년 2월

서울대학교 대학원

생명과학부

김 종 인

지방세포 형태변화에 의한 인슐린 민감도 조절 기전 연구

Roles of lipid droplets in the regulation of insulin-dependent glucose uptake in adipocytes

지도교수 김 재 범

이 논문을 이학박사 학위논문으로 제출함

2019년 2월

서울대학교 대학원

생명과학부

김 종 인

김종인의 박사학위논문을 인준함

2019년 2월

위 원 장 이 건 수 (인)

부위원장 김 재 범 (인)

위 원 구 승 희 (인)

위 원 박 승 범 (인)

위 원 김 진 홍 (인)

Roles of lipid droplets in the regulation of insulin-dependent glucose uptake in adipocytes

A dissertation submitted in partial fulfillment of

the requirement for degree of

DOCTOR OF PHILOSOPHY

To the Faculty of the

School of Biological Sciences

At

SEOUL NATIONAL UNIVERSITY

By

Jong In Kim

February, 2019

Data Approved

Dec. 27th, 2018

ABSTRACT

Roles of adipocyte lipid droplets in the regulation of insulin-dependent glucose uptake

Jong In Kim

Adipose tissue (AT) is a major metabolic organ that regulates energy homeostasis. AT can be largely categorized into visceral white adipose tissue, subcutaneous white adipose tissue, and brown adipose tissue based on anatomical location and functions. The major role of AT is to reserve excess energy sources in lipid droplets (LDs) in form of triglycerides upon nutritional balance. Cellular responsiveness to insulin is defined as “insulin sensitivity”, on the contrary, insufficient response to insulin provokes “insulin resistance”, and insulin resistance is considered as a key etiology of metabolic diseases.

Under various physiological or pathological conditions, adipocytes accompany dramatic changes in insulin sensitivity and morphology. Given that, ATs are largely divided into adipocytes and stromal vascular cells including various immune cells, and exhibit complex cell-to-cell and tissue-to-tissue interactions, it has been difficult to study intrinsic roles of adipocytes in the regulation of insulin sensitivity in ATs. Thus, this dissertation study has been focused on the relationship

between the morphology/shape and insulin responsiveness of adipocytes, and investigated the mechanism by which alteration of adipocyte morphology could affect its functions, particularly, in insulin sensitivity.

In the first chapter, in order to investigate the mechanism of adipocyte hypertrophy-induced insulin resistance in obesity, I developed *in vitro* hypertrophic adipocyte model system by challenging with various free fatty acids to differentiated 3T3-L1 adipocytes. Unlike long chain saturated- fatty acids-induced hypertrophic adipocytes, mono unsaturated-fatty acid, oleic acid, -induced adipocytes hypertrophy potentially provoked insulin resistance without any influences of inflammatory responses and insulin signaling cascades. By adopting microscopic approaches, I could determine the insulin sensitivity of adipocytes with several morphologies at the single cell level. Notably, insulin-dependent glucose transporter 4 (GLUT4) translocation to plasma membrane was preferentially impaired in a unilocular hypertrophic adipocyte-specific manner. In addition, I found that cortical filamentous (F)-actin structure was disrupted compared to small and/or multilocular adipocytes.

In the second chapter, to unveil the roles of adipocyte LDs locularity on insulin sensitivity control, I investigated insulin-dependent GLUT4 trafficking and glucose uptake ability in 1) oleic acids-induced hypertrophic adipocytes with unilocular and enlarged LDs, and 2) reversibly multilocularized adipocytes from oleic acids-induced hypertrophy. The extents of insulin-dependent GLUT4 trafficking and glucose uptake were improved in most physiological conditions when LDs were

multilocularized and reduced in their size. On the contrary, physiological or pathological conditions that exhibited LDs unilocularization and LD enlargement decreased insulin-dependent GLUT4 translocation and glucose uptake of adipocytes. From these observations, I propose novel roles of F/G-actin dynamics as a modulator of insulin-dependent glucose uptake upon different morphologies of adipocytes.

In this study, I discovered followings that 1) adipocyte hypertrophy *per se* provoked insulin resistance via impaired GLUT4 trafficking, independent of inflammatory responses, 2) LDs multilocularization and decrease in their sizes lead to increase the ratio of F/G-actin dynamics, accompanied with improved insulin sensitivity, while 3) LD unilocularization and increase in LD size downregulated the ratio of F/G-actin dynamics, concurrently with impaired insulin sensitivity. Collectively, these data clearly suggest that morphological changes of LDs could affect insulin sensitivity of adipocytes in a cell autonomous manner. I believe that this research provides a new insight that adipocytes morphology and their dynamic regulation plays important roles in the regulation of insulin sensitivity upon nutritional status.

Key words: Adipocyte, Lipid droplet, Actin cytoskeleton, GLUT4, Insulin sensitivity, glucose uptake

Student number: 2009-20326

TABLE OF CONTENTS

LIST OF FIGURES

LIST of TABLES

BACKGROUND

1. Obesity, adipose tissue remodeling, and insulin resistance

1) Obesity and insulin resistance

Obesity is a condition that is medically negative due to excessive accumulation of body fat (*WHO*. January 2015). Obesity is induced by various conditions such as excessive food intake, lack of physical activity, and genetic susceptibility. For the sake of convenience, obesity is defined by the body mass index (BMI), a measurement that divides the weight of a person by the square of the height, over 30 kg/m^2 and overweight is in the range of BMI 25-30 kg/m^2. For decades, the link between obesity and type 2 diabetes has been well recognized.

Insulin resistance commonly refers to reduced glucose lowering effects of insulin. Insulin resistance in obesity and type 2 diabetes is manifested by decreased insulin-dependent glucose transport and metabolism in adipocytes and skeletal muscle and by impaired suppression of hepatic glucose production[1,2]. Insulin resistance is a fundamental risk factor for type 2 diabetes and is also associated with various metabolic disorders including hypertension, hyperlipidemia, and atherosclerosis[3,4]. Although, it has been well established

that increased adiposity is a potential etiology of insulin resistance, the molecular mechanisms by which increased adiposity would cause systemic insulin resistance are not yet clearly understood.

2) Adipose tissue remodeling

Adipose tissue is a caloric reservoir playing an important role in the regulation of systemic energy homeostasis. In response to excessive nutritional state, adipose tissue stores excess energy sources in the form of neutral lipids, whereas in nutritional deprivation, it supplies energy sources to other tissues via lipolysis[5]. In obesity, adipose tissues dynamically increase the size (hypertrophy) and/or number (hyperplasia) of adipocytes. Also, obese adipose tissue suffers from pro-inflammatory responses with inflammatory tones in stromal vascular cells (SVCs) including macrophages, T-cells, and B-cells. These series of events are called “adipose tissue remodeling”, and are known to cause obesity-induced insulin resistance[6]. Because of these intricate events of adipose tissue remodeling in obesity, the intrinsic roles of adipocytes on insulin resistance have not been thoroughly studied.

2. Adipocyte and glucose homeostasis

1) White and brown adipocytes

Adipocytes are specialized cells to store energy sources in lipid droplets (LDs) and are primarily compose adipose tissue[7]. During development, adipocytes are originated from mesenchymal stem cells and differentiated through adipogenesis. There are, at least, two types of adipocytes, white adipocyte and brown adipocyte, compose anatomically different white adipose tissue and brown adipose tissue, respectively. Recently, the existence of beige/brite adipocytes whose gene expression pattern distinct from white or brown adipocytes has been reported.

Mature white adipocytes usually contain one large (unilocular) LD surrounded by a single phospholipid layer. In adipocytes, the stored LDs contain semi-liquid lipid metabolites, mainly composed of triglycerides and cholesteryl esters. Since large LDs in adipocytes occupy most cytoplasm, large white adipocytes have small amounts of cytoplasm (Fig. 1). Accumulating data have shown that white adipocytes secrete a variety of hormones called adipokines, such as leptin, adiponectin, and resistin, that regulate systemic energy metabolism in an endocrine manner.

Morphologically, brown adipocytes contain multiple small (multilocular) LDs and are bumpy in their shape. As well as the LD locularity,

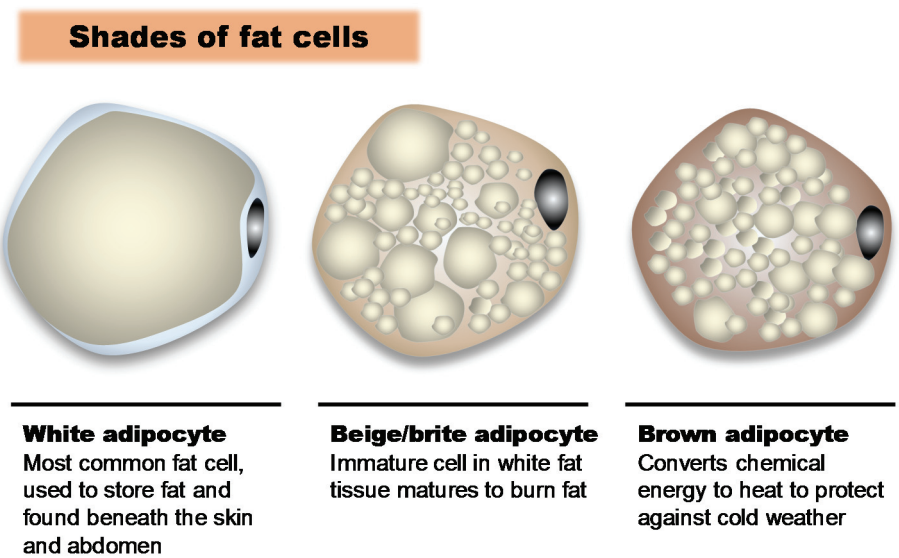

Figure 1. Characteristics of adipocytes. Most white adipocytes have a single lipid droplet (unilocular) and act primarily as energy reservoirs. Beige/brite and brown adipocytes can produce heat (non-shivering thermogenesis) through fat burning and are activated by adrenergic stimuli such as cold stimulation or exercise.

brown adipocytes have plenty of mitochondria, compared to white adipocytes (Fig. 1)[8]. The brown color comes from the large quantity of mitochondria. Mitochondria from brown adipocyte have a large amount of protein called uncoupling protein 1 (UCP1) which is a proton transporter in the inner mitochondrial membrane and acts as an uncoupler of mitochondrial respiratory chain[9,10]. More importantly, brown adipocytes can produce heat (non-shivering thermogenesis) by fuel oxidation. However, in spite of these profound morphological differences, little is known about the effect of LD locularity on adipocytes functions such as insulin sensitivity.

2) Insulin action in adipocytes

Insulin is a key anabolic hormone for whole body energy homeostasis. Adipocytes are one of the most highly insulin-responsive cell types. Insulin promotes adipocyte triglyceride storage by increasing glucose transport and triglyceride synthesis (lipogenesis), and inhibiting lipolysis (Fig. 2)[2]. However, in obesity-induced insulin resistance, decreased insulin-dependent glucose uptake may result, in part, from impaired insulin signaling and/or downregulation of glucose transporter 4 (GLUT4)[11]. Other mechanisms also contribute to insulin resistance in obesity. For instance, in morbid obesity, even though GLUT4 expression is normal,

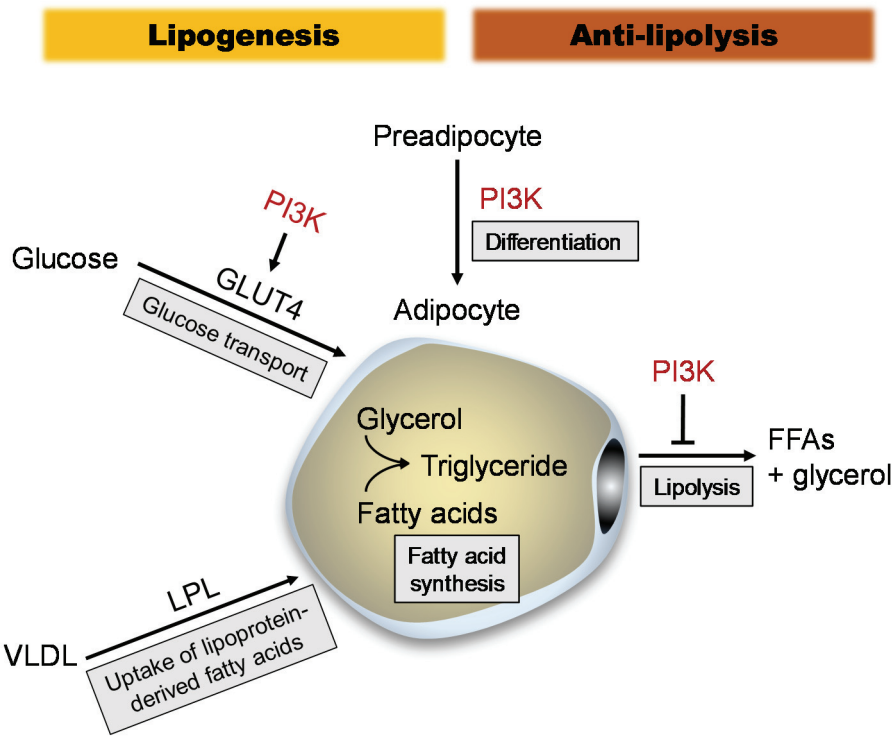

Figure 2. Pleotropic effects of insulin to promote fat storage. Insulin stimulates differentiation of adipocytes. In adipocytes, insulin-induced PI3K-Akt activation promotes lipogenesis through glucose and fatty acid uptake. Many metabolic pathways are regulated by PI3K signaling cascade.

dysregulation of glucose transport appears to be attributable to impair translocation, docking, and/or fusion of GLUT4-containing vesicles (GSVs) with plasma membrane[12,13]. To date, the underlying mechanisms by which adipocyte hypertrophy could affect GLUT4 trafficking remain elusive.

3. Purpose of this study

Adipocyte is one of the most important professional cell types regulating systemic energy homeostasis. Increased adiposity in obesity has been implicated in one of major causes of impaired insulin sensitivity. Nevertheless, because of the complex phenomena such as inflammation resulting from the interaction of adipocytes with SVCs including various immune cells in adipose tissue, the significance of adipocyte-autonomous roles in obesity-induced insulin resistance has not been fully understood. Although it has been considered that adipocyte hypertrophy is associated with detrimental aspects of adipocyte function including insulin sensitivity, the underlying mechanisms how morphological changes of adipocytes affect insulin sensitivity are largely unknown.

In this study, I have investigated the insulin responsiveness according to the changes of LD size and locularity, which could directly affect adipocyte

size and morphology/shape, which would decipher the association of adipocyte morphology and function in a cell-autonomous manner.

In the first chapter, I have established an *in vitro* hypertrophic adipocyte model system by treating various free fatty acids to fully differentiated 3T3-L1 adipocytes. With these hypertrophic adipocytes, I have tested the effects of adipocyte hypertrophy on insulin resistance with the exclusion of any association with other cells. As a readout for the degree of adipocyte insulin sensitivity, insulin-dependent glucose uptake ability was measured by various methods. Notably, I found that hypertrophic adipocytes could provoke insulin resistance in an inflammation independent manner. Consistent with *in vitro* data, high-fat diet (HFD)-fed immunocompromised mice showed obesity-induced systemic insulin resistances independent of adipose tissue inflammation. By using microscopic approaches, I also demonstrated that over-growth of unilocular LD in adipocytes led to reduced insulin-dependent glucose uptake ability in adipocytes, at least partly, via impaired GLUT4 trafficking.

In the second chapter, to further investigate the role of LD number (locularity) in the regulation of adipocyte insulin sensitivity, I have reversed unilocular hypertrophic adipocytes into multilocular adipocytes and measured their insulin-dependent glucose uptake abilities. Intriguingly, when compared to unilocular hypertrophic adipocytes, morphologically reversed multilocular

adipocytes recovered their insulin sensitivity by elevating insulin-dependent GLUT4 trafficking ability. Consistent with this *in vitro* findings, multilocular brown adipocytes isolated from brown adipose tissue showed a higher level of insulin-dependent glucose uptake ability compared to unilocular white adipocytes. I also found that the ratio of filamentous (F)- to globular (G)-actin was dramatically changed by LD locularity. These observations indicate that there might be a strong involvement of actin dynamics in the relationship between cell morphology and GLUT4 trafficking in adipocytes. Taken together, I would like to propose that adipocytes morphology represented by LD size and locularity affects GLUT4 trafficking, accompanied with modulation of actin dynamics and is an important aspect in understanding the physiology and pathology of adipose tissue.

CHAPTER ONE:

Lipid-overloaded enlarged adipocytes provoke insulin resistance independent of inflammation

ABSTRACT

In obesity, adipocyte hypertrophy and pro-inflammatory responses are closely associated with the development of insulin resistance in adipose tissue. However, it is largely unknown whether adipocyte hypertrophy *per se* might be sufficient to provoke insulin resistance in obese adipose tissue. Here, I demonstrate that lipid overloaded hypertrophic adipocytes are insulin resistant independent of adipocyte inflammation. Treatment with saturated or monounsaturated fatty acids resulted in adipocyte hypertrophy, but pro-inflammatory responses were only observed in adipocytes treated with saturated fatty acids. Regardless of adipocyte inflammation, hypertrophic adipocytes with large and unilocular lipid droplet (LD) exhibited impaired insulin-dependent glucose uptake, associated with defects in GLUT4 trafficking to the plasma membrane. Moreover, toll-like receptor 4 mutant mice (C3H/HeJ) with high fat diet-induced obesity were not protected against insulin resistance, although they were resistant to adipose tissue inflammation. Together, my data suggest that adipocyte hypertrophy alone would be crucial to cause insulin resistance in obesity.

INTRODUCTION

Adipose tissue is a key energy storage organ that regulates whole body energy homeostasis. Its parenchymal function is storing excess energy in the form of triglycerides and, is converting them into free fatty acids and glycerol to provide energy upon demand. In addition, as an endocrine organ, adipose tissue synthesizes various adipokines that affect food intake, insulin sensitivity, and immune response[14]. In obesity, adipose tissue expands as a result of increases in adipocyte size (hypertrophy) and adipocyte number (hyperplasia) and actively modulates the population of immune cells[15,16].

Obese subjects exhibit pro-inflammatory responses, ER stress, hypoxia, and/or mitochondrial defects as a result of unbalanced energy inputs in adipose tissue, leading to consequent systemic insulin resistance[17-19]. In obese adipose tissue, chronic and low-grade inflammation have been implicated in insulin resistance, with elevated $F4/80^+$, $CD11b^+$, and $CD11c^+$ M1-like macrophages[20,21]. M1-like macrophages secrete various cytokines that impair insulin sensitivity through the induction of pro-inflammatory signaling, including activation of JNK or NF-κB. Furthermore, several animal models with genetic ablation of pro-inflammatory responses, such as JNK knockout mice and IKK-β heterozygous mice, are resistant to diet-induced obesity and/or insulin resistance because of decreased inflammation[22-25].

Since most metabolic complication studies have been performed using severe and relatively late stage obese models, it is not fully understood which factors or cell types in adipose tissues are primarily responsible for insulin resistance at the early stage of obesity. Recently, I and others have reported that body weight, adipose tissue mass, adipocyte hypertrophy, adipose tissue inflammation, and insulin resistance would increase in mice fed short-term (less than 1 week) high-fat diet (HFD)[26-30]. Interestingly, depletion of macrophages or lymphocytes by clodronate treatment or RAG1 knockout mice did not attenuate insulin resistance in early obesity[28]. These data imply that not only adipose tissue immune cells but also adipocyte changes including adipocyte hypertrophy may play a key role in the initiation of insulin resistance during early obesity. In addition, intima media thickness (IMT), which is a prediction marker of cardiovascular events and strongly associated with insulin resistance[31], was increased with severe obesity but was not influenced by the degree of systemic inflammation or adipose tissue macrophage accumulation[32]. Very recently, it has been reported that early B cell factor 1 (EBF1) reduction caused adipocyte hypertrophy and insulin resistance but did not influence the inflammatory pathways in both mouse and human adipocytes[33]. These emerging evidences have suggested that adipose tissue inflammation, which is one of the major factors of insulin resistance in severe obesity, might be dissociated from adipocyte hypertrophy linked insulin resistance in certain conditions of obesity. Although various studies have suggested a close

relationship between adipocyte hypertrophy, insulin resistance, and inflammation in obesity[34,35], it is largely unclear whether enlarged adipocyte *per se* would initiate insulin resistance regardless of inflammation in obesity.

In this study, I have developed an adipocyte hypertrophy model with or without inflammatory responses and investigated the effects of adipocyte hypertrophy on insulin resistance. Collectively, my data suggest that adipocyte hypertrophy is sufficient to provoke insulin resistance, independent of a pro-inflammatory response, in early obesity.

MATERIALS AND METHODS

Animals and treatments.

7-week-old male C3H/HeN, C3H/HeJ, *db/+*, *db/db*, and C57BL/6J mice were obtained from Central Lab Animal Inc. (Seoul, South Korea). All mice were maintained under specific pathogen-free conditions and were housed in solid-bottom cages with wood shavings for bedding in a room maintained at 25°C with a 12:12-hour light:dark cycle (lights on at 07:00). After a stabilization period of at least 1 week, mice (8 weeks old) were fed a normal chow diet (NCD) until they were fed a 60% high fat diet (HFD) for the indicated times (Research Diets, Inc., NJ). The HFD mice were compared with age-matched chow-fed mice. The average initial body weights in each group of mice were not different. For the oral glucose tolerance test, the mice were fasted for 6 hours, basal blood samples were taken, and glucose was injected orally (2 g/kg). Blood samples were drawn at 15, 30, 45, 60, 90, and 120 minutes after injection. For treatment with rosiglitazone, 12-week-old *db/+*, and *db/db* mice were injected with rosiglitazone (oral gavage, 15 mg/kg/day, Sigma-Aldrich, MO) for 1 month. All animal procedures were in accordance with the research guidelines for the use of laboratory animals of Seoul National University.

Cell culture.

3T3-L1 preadipocytes were grown to confluence in Dulbecco's modified

Eagle's medium (DMEM) supplemented with 10% bovine calf serum (BCS; Invitrogen Life Technologies, Carlsbad, CA). 2 days after the cells reached confluence (day 0), differentiation of the 3T3-L1 cells was induced in DMEM containing 10% fetal bovine serum (FBS; Invitrogen Life Technologies, Carlsbad, CA), methylisobutylxanthine (520 μM), dexamethasone (1 μM), and insulin (167 nM) for 48 hours. The culture medium was replaced on alternate days with DMEM containing 10% FBS and 167 nM insulin.

Free fatty acid treatment.

Free fatty acids (FFA) (Sigma-Aldrich, MO) were conjugated with FFA-free bovine serum albumin (BSA) for administration to cells. Briefly, FFAs were dissolved in ethanol and diluted in DMEM containing 1% FBS and 2% (w/v) BSA for 10 minutes at 55°C. BSA conjugated FFAs containing media were challenged to cells.

Quantitative RT-PCR

Total RNA was isolated from 3T3-L1 adipocytes, and epididymal white adipose tissues (eWATs). cDNA was synthesized using the M-MuLV reverse transcriptase kit according to the manufacturers' instructions (Thermo Fisher Scientific, MA). The primers used for quantitative real-time PCR were obtained from Bioneer (South Korea), and their sequences are provided in Table 1.

Western blot analysis

3T3-L1 adipocytes were stimulated with or without 10 nM insulin for 20 minutes at 37°C. 3T3-L1 adipocytes were lysed with NETN buffer (20 mM Tris [pH 7.9], 1 mM EDTA, 100 mM NaCl, 0.5% NP-40, 1 mM Na_3VO_4, 100 mM NaF, and protease inhibitor cocktail tablets [Roche Diagnostics]). Total cell lysates were centrifuged at 12,000 rpm at 4°C for 15 minutes to remove fat debris. The protein concentration was determined using a BCA assay kit (Pierce). Western blot analyses were conducted according to the manufacturer's protocol (Cell Signaling Technology). IκBα, IRS1, Akt/PKB, and phospho-Akt/PKB antibodies were purchased from Cell Signaling Technology; GSK3β and phospho-GSK3β antibodies were from Transduction Laboratories; and the phospho-IRS1 antibody was from Biosource; p65 antibody was from Santa Cruz Biotechnology; Lamin B was from ab frontier; GAPDH antibody was from BD Biosciences.

Glucose uptake assay

3T3-L1 adipocytes were incubated in low-glucose DMEM containing 0.1% BSA for 16 hours at 37°C. Cells were stimulated with or without 100 nM insulin for 20 minutes at 37°C. Glucose uptake was initiated by the addition of [^{14}C]-

GENE	FORWARD PRIMER	REVERSE PRIMER
Adiponectin	5'-GGCAGGAAAGGAGAACCTGG-3'	5'-AGCCTTGTCCTTCTTGAAGA-3'
aP2	5'-AAGAAGTGGGAGTGGGCTTT-3'	5'-GCTCTTCACCTTCCTGTCGT-3'
ATGL	5'-TATCCGGTGGATGAAAGAGC-3'	5'-CAGTTCCACCTGCTCAGACA-3'
BIP/GRP78	5'-ACTTGGGGACCACCTATTCC-3'	5'-TTTCTTCTGGGGCAAATGTC-3'
CD11b	5'-GACTCAGTGAGCCCCATCAT-3'	5'-AGATCGTCTTGGCAGATGCT-3'
CD11c	5'-CTGGATAGCCTTTCTTCTGC-3'	5'-GCACACTGTGTCCGAACTC-3'
CD36	5'-GAGCAACTGGTGGATGGTTT-3'	5'-GCAGAATCAAGGGAGAGCAC-3'
Cyclophilin	5'-CAGACGCCACTGTCGCTTT-3'	5'-TGTCTTTGGAACTTTGTCTG-3'
FAS	5'-GCCTACACCCAGAGCTACCG-3'	5'-GCCATGGTACTTGGCCTTG-3'
FATP1	5'-GGGAAGAGCCTCCTCAAGTT-3'	5'-TACCTGCTGTGCACCACAAT-3'
GLUT4	5'-GATTCTGCTGCCCTTCTGTC-3'	5'-ATTGGACGCTCTCTCTCCAA-3'
HSL	5'-GGAGCACTACAAACGCAACGA-3'	5'-TCGGCCACCGGTAAAGAG-3'
IL-6	5'-AGTTGCCTTCTTGGGACTGA-3'	5'-TCCACGATTTCCCAGAGAAC-3'
PERILPIN	5'-CACACCGTGCAGAACACTCT-3'	5'-CCTCTGCTGAAGGGTTATCG-3'
PPARα	5'-ATGCCAGTACTGCCGTTTTC-3'	5'-GGCCTTGACCTTGTTCATGT-3'
PPARγ	5'-TCACAAGAGCTGACCCAATGG-3'	5'-GGCTCTACTTGATCGACTTTG-3'
RANTES	5'-CATATGGCTCGGACACCACT-3'	5'-CTCTGGGTTGGCACACACTT-3'
SAA	5'-AGCGATGCCAGAGAGGCTGT-3'	5'-ACCCAGTAGTTGCTCCTCTT-3'
SREBP-1c	5'-GGAGCCATGGATTGCACATT-3'	5'-CAGGAAGGCTTCCAGAGAGG-3'
TLR4	5'-CAGTGGTCAGTGTGATTGTG-3'	5'-TTCCTGGATGATGTTGGCAG-3'
TNFα	5'-CGGAGTCCGGGCAGGT-3'	5'-GCTGGGTAGAGAATGGATCA-3'
VEGF	5'-GGAGATCCTTCGAGGAGCAC-3'	5'-GGCGATTTAGCAGCAGATATA-3'

Table 1. List of qPCR primer sequences

deoxyglucose at a final concentration of 3 mol/l for 10 minutes in HEPES-buffered saline (140 mM NaCl, 5 mM KCl, 2.5 mM $MgCl_2$, 1 mM $CaCl_2$, and 20 mM HEPES [pH 7.4]). The reaction was terminated by separating the cells from HEPES-buffered saline and [^{14}C]-deoxyglucose. After washes in ice-cold PBS, the cells were extracted using 0.1% SDS, and scintillation counting was used to measure ^{14}C radioactivity. The protein concentration was determined, and the radioactivity was normalized to the protein concentration.

***In vitro* glucose bioprobe uptake assay**

3T3-L1 adipocytes were cultured on an 8-well chamber plate (Lab-Tek II). After differentiation, the cell culture medium was changed to a low-glucose medium (without FBS), and the cells were maintained in the new medium for 4 hours. The cells were then incubated for 1 hour in glucose-deficient DMEM (without FBS). For continuous monitoring of cellular glucose uptake with a DeltaVision imaging system (GE Healthcare), the 8-well chamber plate was loaded on the stage of the microscope. After pretreatment with 5 μm GB-Cy3[36], 100 nM insulin was administered. Fluorescence images were recorded every 2 minutes. The images were digitized and saved on a computer for further analysis. The temperature of the chamber was maintained at 37°C.

Ex vivo glucose bioprobe uptake assay

Adipose tissues were removed and sliced into sections of 5 × 5 × 2 mm. Sliced samples were incubated in low-glucose DMEM containing 0.1% BSA for 30 minutes at 37°C. Sliced samples were incubated with 50 μM GB-Cy3 for 30 minutes in the presence or absence of 1 μM insulin. After several washes with PBS-Tween 20, the adipocytes were stained with fluorescein isothiocyanate-conjugated BODIPY. The samples were then stained with Vectashield solution (Vector Labs Inc.) containing 4′,6-diamidino-2-phenylindole (DAPI) and observed using a Zeiss LSM 700 confocal microscope (Carl Zeiss).

Total internal reflection fluorescence microscopy

TIRFM imaging was performed using an inverted microscope system equipped with a 100× 1.45 NA (numerical aperture) objective (Nikon). Images were collected using the NIS-Elements AR software. All experiments were performed at room temperature (22–25°C).

Statistical analysis

Results represent data from multiple (three or more) independent experiments. Error bars represent standard deviation, and *P* values were calculated using Student's t-test or ANOVA.

RESULTS

Treatment with long-chain fatty acids induces adipocyte hypertrophy

To characterize hypertrophic adipocytes, I developed a cell culture model of adipocyte hypertrophy. Differentiated 3T3-L1 adipocytes were challenged for 6 days with saturated fatty acids (SFAs) (palmitic acid, C16:0 and stearic acid, C18:0) and a monounsaturated fatty acid (MUFA) (oleic acid, C18:1) that are abundantly present in the diet[37,38]. Long-chain fatty acid-treated adipocytes became enlarged in time- and dose-dependent manners (Fig. 3A). Oil red O staining revealed that lipid-overloaded hypertrophic adipocytes contained enlarged unilocular-like LDs (Fig. 3B).

MUFA-challenged hypertrophic adipocytes lack inflammatory responses

Given that saturated fatty acids upregulate pro-inflammatory pathways[39,40], I asked whether SFA-treated or MUFA-treated adipocytes would exhibit different inflammatory responses. Similar to TNFα-treated adipocytes, SFAs-induced hypertrophic adipocytes showed increased nuclear NF-κB (p65), JNK phosphorylation, and decreased cytosolic IκBα (Fig. 4A). However, MUFA-induced hypertrophic adipocytes did not significantly alter pro-inflammatory signaling cascades, unlike SFAs-induced hypertrophic adipocytes. As shown in Fig. 4B, the mRNA levels of

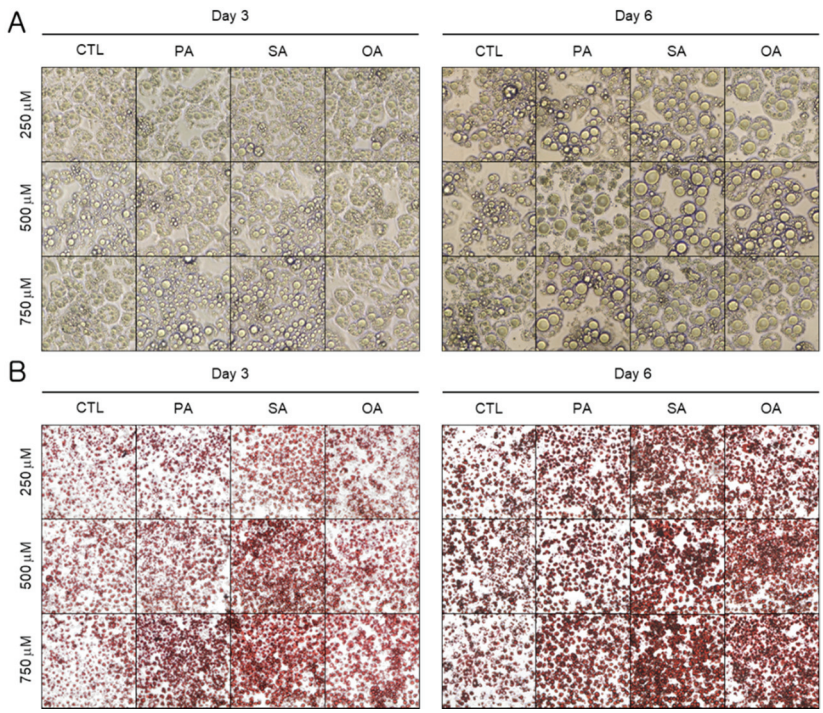

Figure 3. Long-chain fatty acids-induce adipocyte unilocularization and hypertrophy. 3T3-L1 adipocytes were differentiated and then cultured for another 6 days with various long-chain fatty acids at the indicated doses (250, 500, and 750 μM). CTL, control (BSA); PA, palmitic acid; SA, stearic acid; OA, oleic acid. (A) Microscopic images were obtained on the indicated days. (B) Oil red O staining of 3T3-L1 adipocytes treated with various fatty acids.

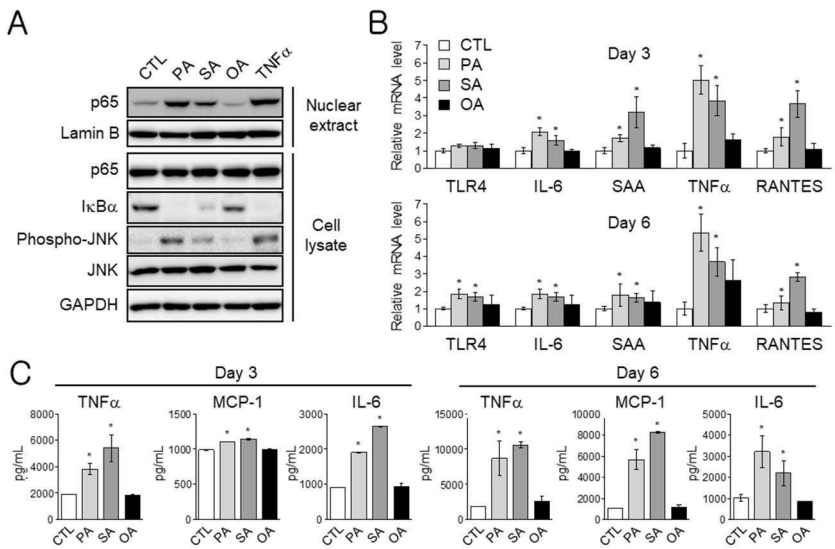

Figure 4. SFA-treated adipocytes, but not MUFA-treated adipocytes, promote pro-inflammatory responses. (A) After treatment of 3T3-L1 adipocytes with various long-chain fatty acids (500 μM), nuclear extracts and cell lysates were subjected to immunoblot analysis. TNF-a concentration, 10 ng/ml. (B) mRNA levels of pro-inflammatory genes. *, P< 0.05 versus CTL cells (Student's t test). (C) Levels of TNF-α, MCP-1, and IL-6 secreted from lipid-overloaded adipocytes. *, P< 0.05 versus CTL cells (Student's t test).

pro-inflammatory cytokines such as IL-6, SAA, TNFα, and RANTES were elevated in SFAs-treated adipocytes but not in MUFA-treated adipocytes. To assess whether the gene expression profiles of lipid-overloaded adipocytes were linked with cytokine secretion, ELISA and chemotaxis assay were performed. As expected, conditioned media from SFAs-treated adipocytes contained higher levels of pro-inflammatory cytokines including TNFα, MCP-1 and IL-6 than conditioned media from control adipocytes or MUFA-treated adipocytes (Fig. 4C). Next, to confirm the idea that SFA treatment could indeed potentiate inflammatory responses in hypertrophic adipocytes, chemotaxis assays were performed. The migration of THP-1 monocytes was increased when the cells were incubated with conditioned media from SFAs-treated adipocytes (Fig. 5). In contrast, conditioned media from MUFA-treated adipocytes had little effect on THP-1 migration (Fig. 5). These data indicate that SFA-treated hypertrophic adipocytes tend to be pro-inflammatory, unlike MUFA-treated hypertrophic adipocytes.

Hypertrophic adipocytes are insulin resistant independent of inflammation

To assess insulin sensitivity of hypertrophic adipocyte models, I performed insulin-dependent glucose uptake assays. As shown in Fig. 6A, insulin-dependent glucose uptake was attenuated in hypertrophic adipocytes,

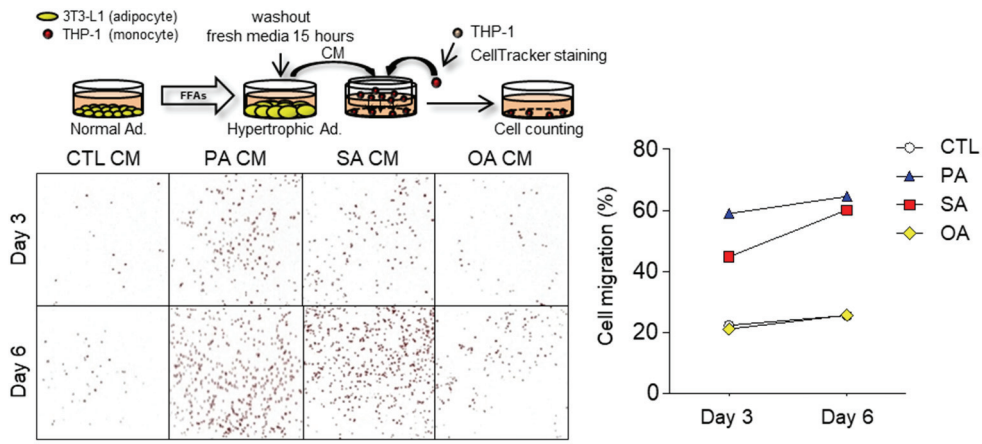

Figure 5. SFA-treated adipocytes, but not MUFA-treated adipocytes, secrete chemoattractant factors. Migration of THP-1 monocytes. THP-1 monocytes were prestained with celltracker (red) and incubated for 6 hr in transwell plates (8 μm pore) with conditioned medium (CM). Photomicrographs of migrated cells were taken (left). Cell migration was assessed (right).

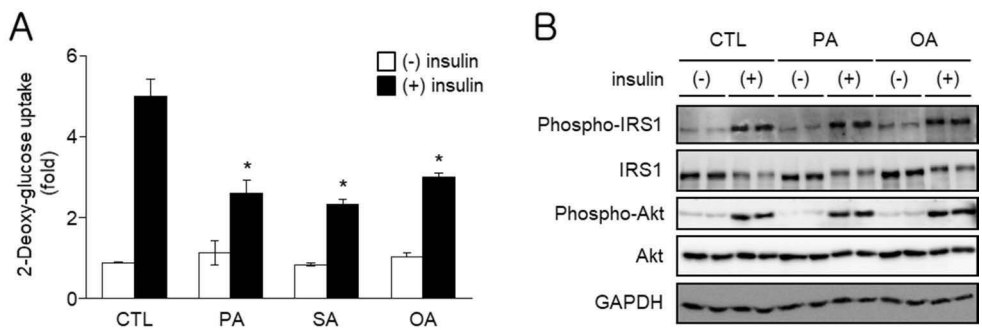

Figure 6. Hypertrophic adipocytes are insulin resistant without any changes in the insulin downstream signaling cascade. 3T3-L1 adipocytes were differentiated and then cultured for another 6 days with various long-chain fatty acids (500 μM). (A) Insulin-dependent glucose uptake assays using [^{14}C]deoxyglucose. *, P< 0.05 versus CTL cells (Student's t-test). (B) Immunoblot analysis of adipocytes treated for 6 days with long-chain fatty acids, with or without insulin (10 nM).

regardless of the kinds of treated fatty acids. Unexpectedly, in SFAs- and MUFA-induced hypertrophic adipocytes, insulin downstream signaling were not different from control cells (Fig. 6B). In addition, when freshly differentiated 3T3-L1 adipocytes were challenged with conditioned media collected from SFA- or MUFA-induced hypertrophic adipocytes, it appeared that there was no significant reduction in insulin signaling cascades (Fig. 7). These data imply that insulin resistance of hypertrophic adipocytes might be dissociated from pro-inflammatory responses.

To explore the potential relationship between adipocyte morphology and insulin resistance, I adopted single cell-based insulin-dependent glucose bioprobe uptake assays[36]. Consistent with radioisotope based insulin-dependent glucose uptake assay (Fig. 6A), glucose bioprobe uptake analysis revealed that SFA- or MUFA-induced hypertrophic adipocytes were insulin resistant (Fig. 8). Compared with control adipocytes, reduced uptake rates of glucose bioprobe were similar in SFAs or MUFA challenged adipocytes (Fig. 8). However, it is of interest to note that some small adipocytes in lipid-overloaded adipocytes showed relatively intense glucose bioprobe signals (Fig. 8). To examine whether insulin-dependent glucose uptake was differentially regulated in response to adipocyte cell size and/or LD morphology in an inflammation independent manner, I classified morphologically heterogeneous populations of MUFA-induced hypertrophic adipocytes into four categories. 1) small/multilocular adipocytes (S/M-ADs), 2) large/multilocular adipocytes

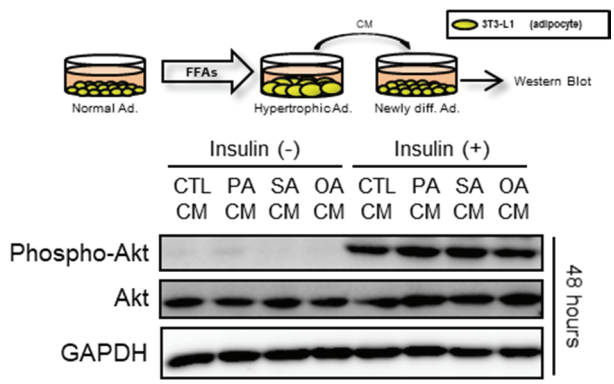

Figure 7. Hypertrophic adipocyte-secreted factors are dissociated with insulin downstream signaling. Conditioned medium was collected from adipocytes overloaded with long-chain fatty acids for 6 days and then treated with newly differentiated 3T3-L1 adipocytes (top). Immunoblot analysis of adipocytes treated with conditioned medium (CM) for 48 h, with or without insulin (10 nM) (bottom).

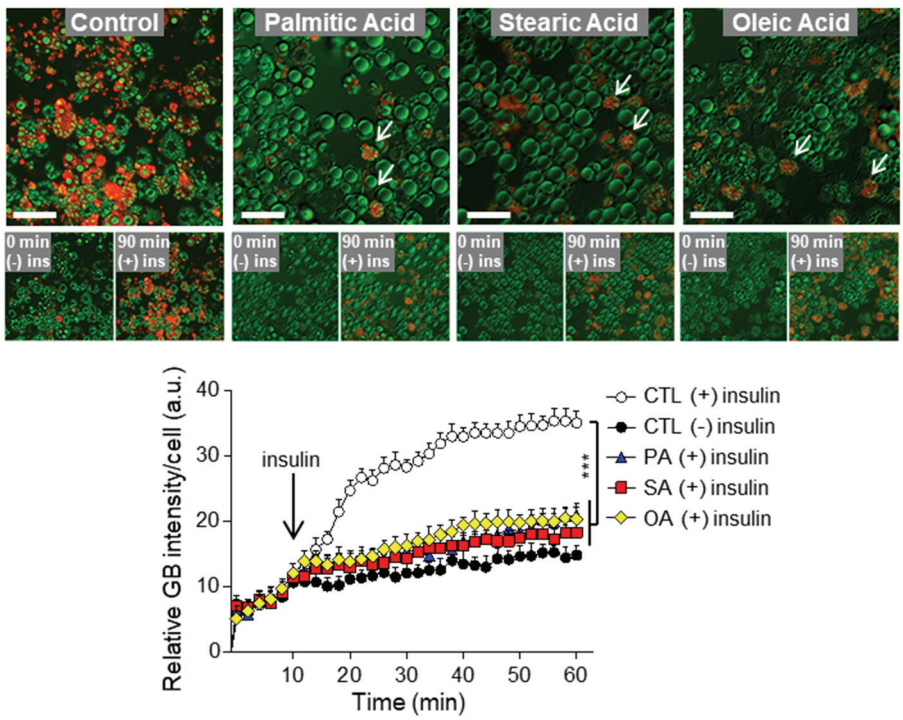

Figure 8. Adipocyte hypertrophy induce insulin resistance. 3T3-L1 adipocytes were differentiated and then cultured for another 6 days with various long-chain fatty acids (500 μM). Hypertrophic adipocytes challenged with fatty acids were incubated with a Cy3-labeled glucose bioprobe. After a 10 min incubation, insulin was added, and the fluorescence intensity of the glucose bioprobe was monitored every 2 min using a DeltaVision imaging system. Arrows designate relatively small adipocytes. Scale bars, 80 μm. ***, $P < 0.001$ versus CTL cells (ANOVA).

(L/M-ADs), 3) small/unilocular-like adipocytes (S/U-ADs), and 4) large/unilocular-like adipocytes (L/U-ADs) (Fig. 9A). As shown in Fig. 9B, the relative portion of L/U-ADs was predominantly increased by both SFAs and MUFA overloaded hypertrophic adipocytes. Single cell based analyses with glucose bioprobe revealed that insulin-dependent glucose bioprobe uptake in S/M-ADs and L/M-ADs were comparably increased after insulin stimulation. While the degree of insulin-dependent glucose bioprobe uptake in S/U-ADs was slightly lower than that of S/M-ADs or L/M-ADs, the level of insulin-dependent glucose bioprobe uptake in L/U-ADs was markedly attenuated (Fig. 9C). Together, these results suggest that adipocyte hypertrophy with unilocular-like LDs would lead to adipocyte insulin resistance in a cell-autonomous manner, independent of inflammatory responses.

Enlarged adipocytes with unilocular-like LDs showed defective GLUT4 trafficking

Unlike SFA-induced hypertrophic adipocytes, MUFA-induced hypertrophic adipocytes did not alter the expression of pro-inflammatory genes (Fig. 4B). Despite of this result, either SFA- or MUFA-induced hypertrophic adipocytes greatly diminished insulin dependent glucose uptake ability (Fig. 6A and 8). Thus, I asked the question whether GLUT4 trafficking might be associated with decreased insulin-dependent glucose uptake in hypertrophic adipocytes. Adipocytes expressing mCherry-GLUT4-Myc were immuno-

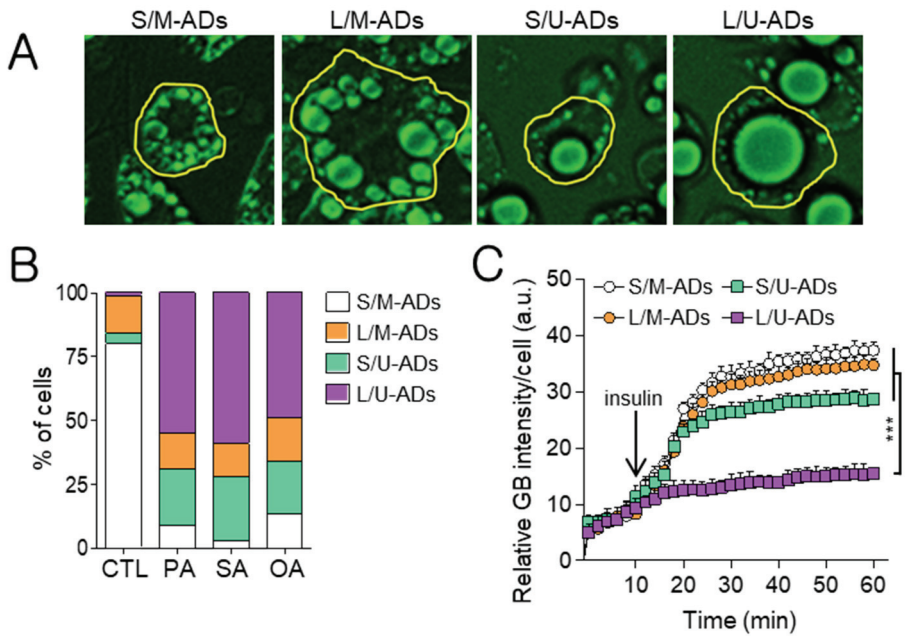

Figure 9. Large/unilocular adipocytes are selectively insulin resistant. 3T3-L1 adipocytes were differentiated and then cultured for another 6 days with OA (500 μM). (A) Hypertrophic adipocytes were categorized into four groups: (i) S/M-ADs, (ii) L/M-ADs, (iii) S/U-ADs, and (iv) L/U-ADs (B) Cellular distributions of each categorized cell type were computationally calculated by using ImageJ. (C) Glucose bioprobe fluorescence intensity in each cell type was detected every 2 min by using DeltaVision imaging system (bottom). ***, P< 0.001 versus CTL cells (ANOVA).

stained with anti-Myc:GFP antibodies, and GLUT4-Myc:GFP signals on the plasma membrane were detected using total internal reflection fluorescence microscopy (TIRFM), in the presence or absence of insulin (Fig. 10A). As shown in Fig. 5B, the amounts of plasma membrane GLUT4 in control adipocytes were increased upon insulin exposure. Interestingly, SFA- or MUFA-treated L/U-ADs decreased GLUT4 plasma membrane translocation in response to insulin exposure (Fig. 10B). In contrast, insulin-dependent GLUT4 translocation was intact in the other types of adipocytes (S/M-ADs, L/M-ADs, and S/U-ADs) (Fig. 10C).

Since it is well known that cytoskeletal proteins are involved in adipogenesis, LD formation, and GLUT4 trafficking[1-3], I hypothesized that cytoskeleton development might be altered in hypertrophic adipocytes containing unilocular-like LDs, thus impeding GLUT4 docking to the plasma membrane. To test this hypothesis, lipid-overloaded hypertrophic adipocytes were stained with phalloidin-TRITC to detect the cellular actin organization. As shown in Fig. 11A, the cytosolic and cortical actin structures were markedly disorganized in L/U-ADs while those of S/M-ADs, L/M-ADs, and S/U-ADs were well organized. Consistent with the pattern of actin organization, insulin-dependent plasma membrane GLUT4 translocation was decreased in L/U-ADs when compared with S/M-ADs, L/M-ADs, and S/U-ADs (Fig. 11B). These data suggest that the reduction of insulin-dependent glucose uptake in hypertrophic adipocytes would be resulted, at least in part, from the dysregulation of cortical

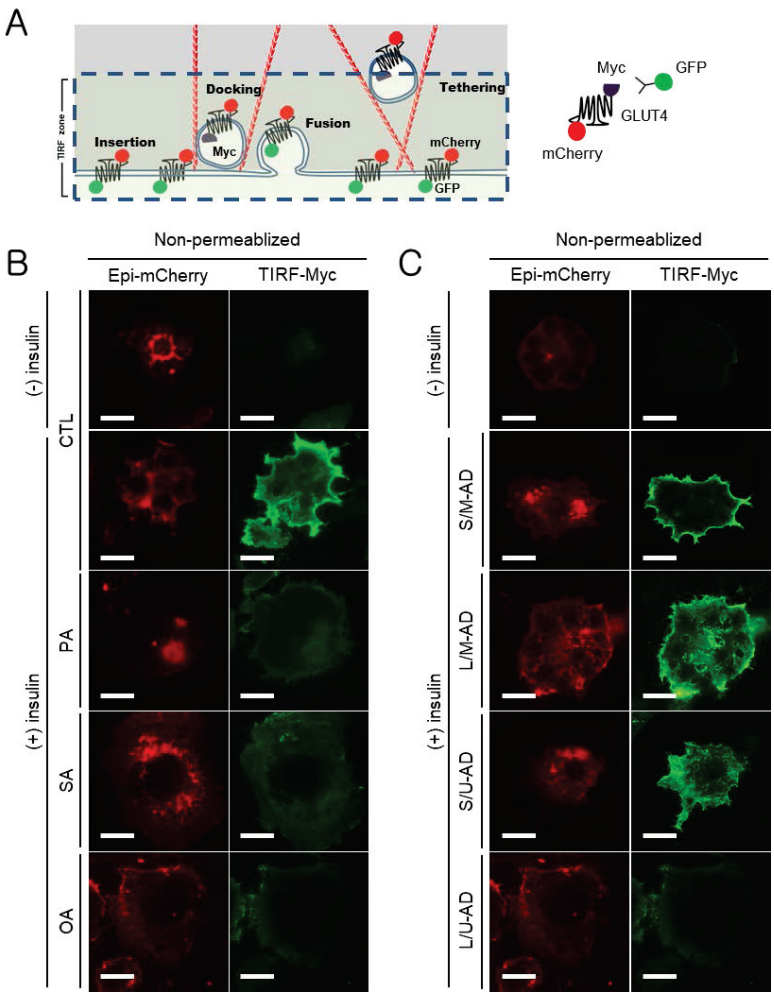

Figure 10. Impaired insulin-stimulated GLUT4 trafficking in large/unilocular adipocytes. (A) Schematic drawing illustrating events observed under the TIRF zone. (B) Insulin-induced GLUT4 membrane insertion was examined by using TIRFM in nonpermeabilized cells. (C) Insulin-induced GLUT4 membrane insertion was examined by using TIRFM in nonpermeabilized cells. Data presented are microscopic images representative of indicated groups. Scale bars, 20 μm.

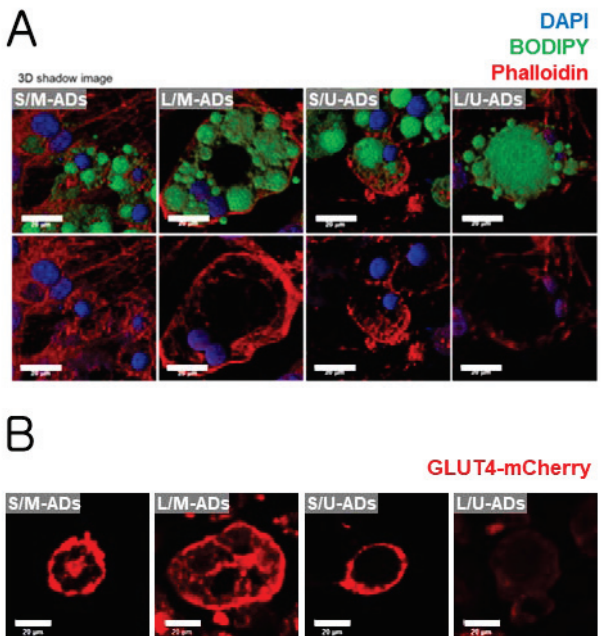

Figure 11. Disruption of cortical F-actin structures in large/unilocular adipocytes. 3T3-L1 adipocytes were treated with OA (500 μM) for 6 days. (A) Cellular F-actin structures. Scale bars, 20 μm. (B) Insulin-stimulated GLUT4 translocation to plasma membrane. Scale bars, 20 μm.

actin remodeling and the consequent impairment of insulin-dependent GLUT4 plasma membrane translocation.

Toll-like receptor 4 (TLR4) mice fed short-term HFD exhibit adipose tissue insulin resistance without adipose tissue inflammation

Pro-inflammatory responses and adipocyte hypertrophy are rapidly induced in early obesity in C57BL/6J mice fed short-term (<1 week) HFD[4-8]. To test whether adipocyte hypertrophy could promote insulin resistance in adipose tissue independent of inflammatory responses, C3H/HeJ TLR4 mutant mice defective in TLR4-dependent inflammation were tested. After 1-week of HFD, body weight gain and the epididymal white adipose tissue (eWAT) mass were increased in both C3H/HeN wild-type control and C3H/HeJ TLR4 mutant mice (Fig. 12A). The adipocytes were also comparably enlarged in control and TLR4 mutant mice upon HFD (Fig. 12B). Unlike HFD-fed control mice, HFD fed TLR4 mutant mice did not show elevated adipose tissue inflammation, despite of adipose tissue expansion (Fig. 12C). To evaluate the systemic insulin sensitivity of control and TLR4 mutant mice, an oral glucose tolerance test was administered. As shown in Fig. 12D and E, both control and TLR4 mutant mice fed HFD were glucose intolerant. To test whether hypertrophic adipocytes induced by short-term HFD feeding might be involved in glucose intolerance, I isolated adipose tissues from control and TLR4 mutant mice and performed *ex vivo* insulin-dependent glucose bioprobe uptake assays. Despite of decreased

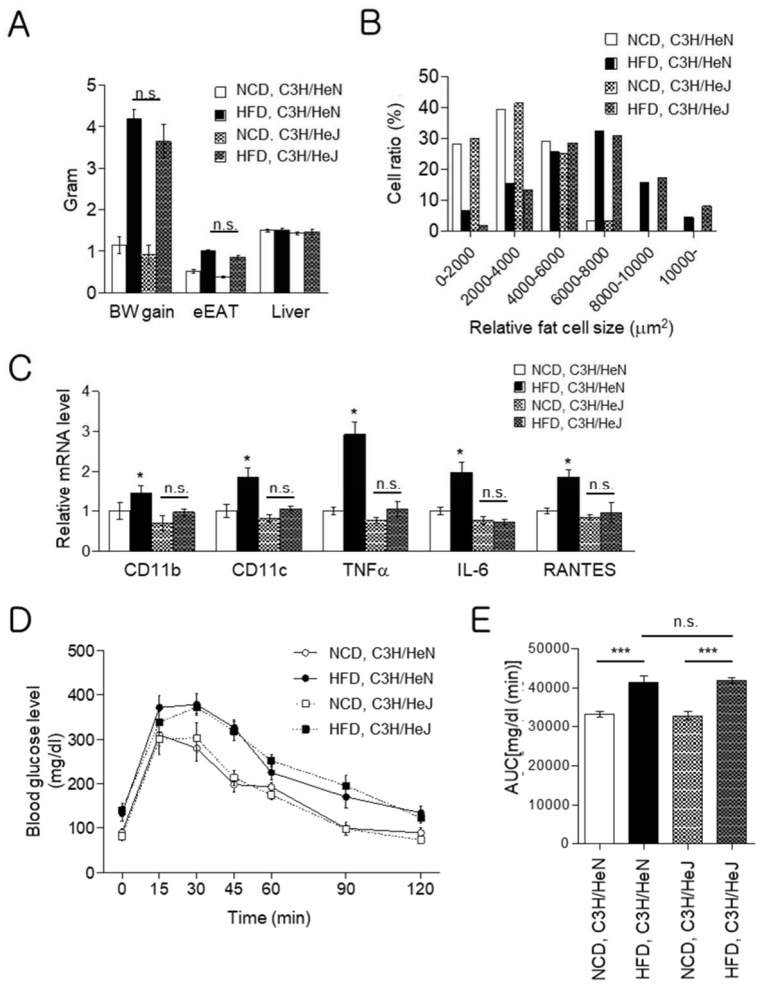

Figure 12. Systemic insulin resistance in short-term HFD-fed TLR4 mutant mice. 10-week-old C3H/HeN and C3H/HeJ mice were fed an NCD or HFD for 1 week. (A) Metabolic parameters. (B) Distribution of adipocyte sizes in eWAT. (C) mRNA levels of inflammatory genes from eWAT. (D and E) Oral glucose tolerance test (D) and area under the curve (AUC). Each bar represents the mean standard deviation (SD) for each group of mice (n=7). *, P< 0.05; ***, P< 0.001; n.s., not significant.

inflammatory responses in adipose tissue of TLR4 mutant mice, the degree of insulin-dependent glucose bioprobe uptake ability in TLR4 mutant mice upon HFD was similar to that of control mice (Fig. 13A and B). Taken together, these results suggest that hypertrophic adipocytes primarily cause adipose tissue insulin resistance in early obesity, independent of adipocyte inflammation.

Rosiglitazone generates small adipocytes and stimulates insulin-dependent glucose uptake

As PPARγ agonists, thiazolidinediones (TZDs) have multiple roles such as insulin sensitization, anti-inflammatory effects, and induction of new adipogenesis in obese animals[43,44]. To determine whether newly differentiated small adipocytes might be more insulin sensitive than nearby hypertrophic adipocytes, rosiglitazone, one of the TZD class of drugs, was administrated orally to obese *db/db* mice. As expected, rosiglitazone restored the mRNA level of adiponectin and insulin signaling accompanied with novel adipocytes differentiation in the adipose tissue of *db/db* mice (Fig. 14A and B). In *db/db* mice, *ex vivo* assays showed that insulin-dependent glucose bioprobe uptake was greatly increased in rosiglitazone-induced, newly differentiated small adipocytes compared to adjacent large adipocytes (Fig. 15). These *in vivo* and *ex vivo* results indicate that hypertrophic adipocytes with large/unilocular LDs in obese adipose tissue are important for the induction of adipose tissue insulin resistance in obesity.

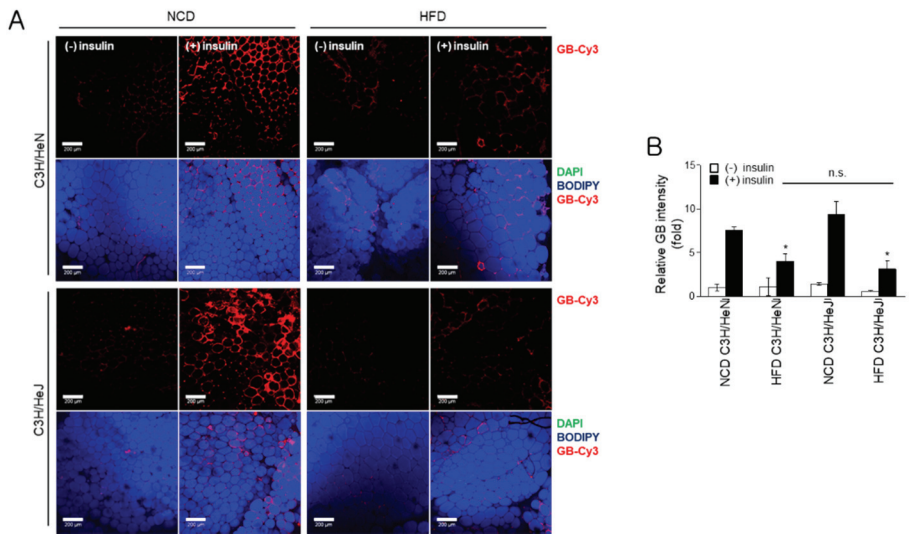

Figure 13. AT insulin resistance in short-term HFD-fed TLR4 mutant mice. eWATs from wild-type control C3H/HeN mice and TLR4 mutant C3H/HeJ mice fed HFD for 1 week were ex vivo cultured. (A and B) Insulin-dependent glucose bioprobe uptake assay. Adipose tissues were *ex vivo* cultured with or without insulin (1 μM). Glucose bioprobe and BODIPY were incubated for 30 min. (A) Glucose bioprobe fluorescence from each group was visualized with confocal microscopy. Scale bars, 200 mm. (B) The relative glucose bioprobe intensity per cell was analyzed using ImageJ. Each bar represents the mean SD for each group of mice (n 7). *, P< 0.05; n.s., not significant.

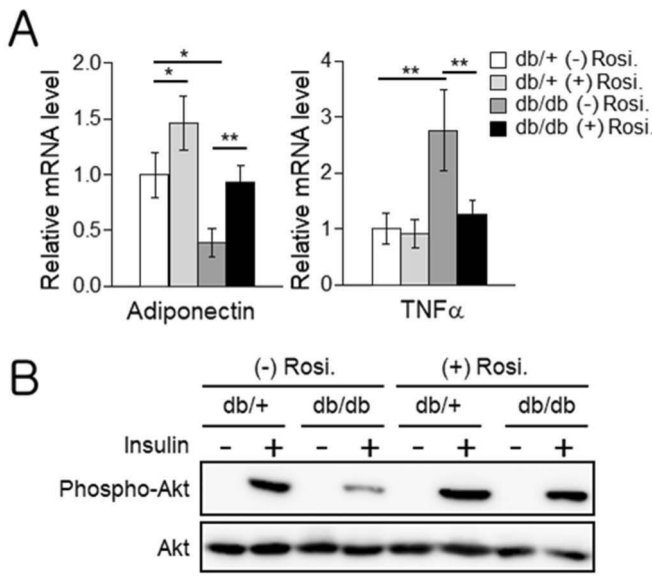

Figure 14. Decreased inflammatory gene expression and improved insulin signaling in *db/db* mice by rosiglitazone treatment. For 1 month, 12-week-old *db/+* and *db/db* mice were treated without or with rosiglitazone (15 mg/kg) by oral gavage. (A) Relative mRNA levels of adiponectin and TNF- from the eWAT of rosiglitazone-treated *db/+* and *db/db* mice. *,P< 0.05; **, P< 0.01. (B) Immunoblot analysis of eWAT. Phosphorylation of Akt (Ser308) with or without insulin (50 nM) treatment.

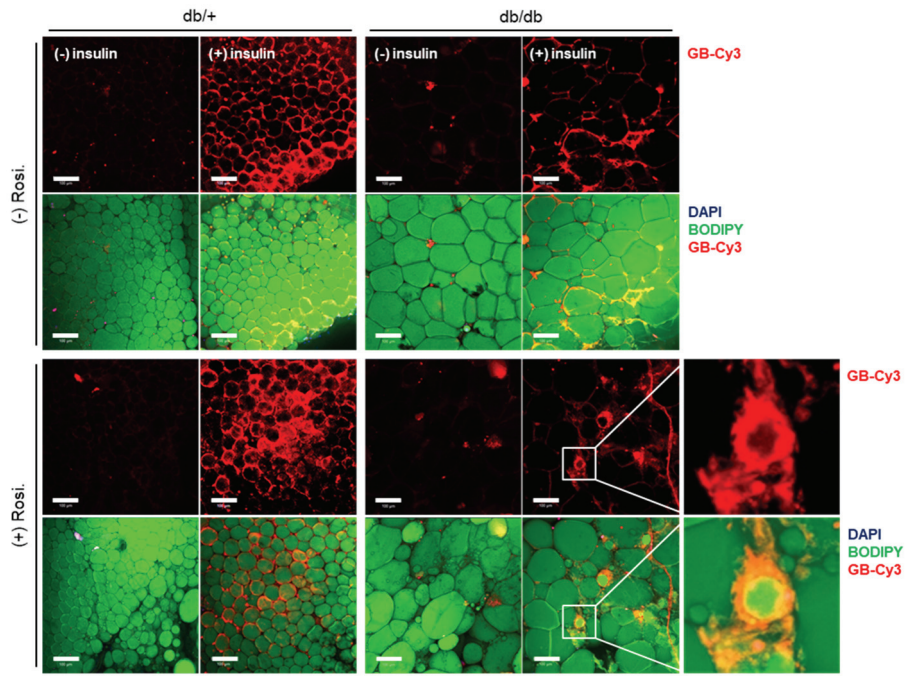

Figure 15. Insulin sensitive small adipocytes in rosiglitazone-treated *db/db* mice. For 1 month, 12-week-old *db/+* and *db/db* mice were treated without or with rosiglitazone (15 mg/kg) by oral gavage. Ex vivo glucose bioprobe uptake assay. eWATs from rosiglitazone-treated *db/+* or *db/db* mice were *ex vivo* cultured with or without insulin (1 M). Scale bars, 100 μm.

DISCUSSION

In obesity, increased adiposity and immune cell infiltration into adipose tissue contribute to insulin resistance in parallel with dysregulation of glucose and lipid metabolism[17,18,20,27]. Given that adipose tissue is composed of various cell types, including endothelial cells, macrophages, lymphocytes, and preadipocytes in stromal vascular factions, as well as adipocytes, it has been difficult to determine whether adipocyte hypertrophy *per se* might induce adipose tissue insulin resistance independent of pro-inflammatory responses in obesity. The recent findings that insulin resistance induced by short-term HFD could occur in the absence of pro-inflammatory responses[27,28,45] propose that adipocyte dysfunction associated with hypertrophy would play a crucial role in the incidence of adipose tissue insulin resistance. In this regard, the characterization of hypertrophic adipocytes is important to decipher the mechanisms of insulin resistance, especially in early obesity. Here, I demonstrated that adipocyte hypertrophy could directly cause insulin resistance in a cell-autonomous manner via dysregulation of cortical actin structures and impairment of GLUT4 trafficking.

Although there are many circumstantial evidences[46-49], the molecular mechanisms of adipocyte hypertrophy-induced insulin resistance are largely unknown. One of the major impediments to investigate hypertrophic adipocytes is the lack of proper model systems *in vitro* and *in vivo*. It is certain that primary

adipocytes would be the best model to study adipocyte hypertrophy. However, there are several technical obstacles to use primary adipocytes as a representative of hypertrophic adipocytes model system. First, large primary adipocytes are physically and chemically fragile. Because of the weakness, collagenase digestion and isolation steps might decrease significant portions of large adipocytes. Second, primary adipocytes cannot be free from contamination of stromal vascular cells. In adipose tissue, adipocytes and other cell types including macrophages and T-cells are physically stuck together. In this regard, isolating "pure adipocytes" free from stromal cell contamination is not technically feasible[46,49]. Third, since primary adipocytes were floating in cell culture conditions, it is not technically practical to carry out various *in vitro* experiments. Thus, I have utilized 3T3-L1 adipocytes as an alternative approach to investigate adipocyte morphology and its functions. Although differentiated 3T3-L1 adipocytes exhibit differences from *in vivo* adipocyte such as multilocular LDs and lower responsiveness to LPS, it appears that 3T3-L1 adipocyte has its own merits as a "pure" fat cell model without the influences of other cells composed in adipose tissue.

To mimic insulin resistance *in vitro*, 3T3-L1 adipocytes have been challenged with glucose oxidase, chronic insulin, TNF-α, dexamethasone, or various free fatty acids[50-52]. However, because these protocols have been used to study the relatively acute effects of the stimuli on adipocyte function, they failed to reveal the roles of adipocyte hypertrophy and LD locularity. To

overcome these limitations, I assessed the time- and dose-dependent effects of long-chain fatty acid treatment on 3T3-L1 adipocytes and optimized the conditions to generate hypertrophic adipocytes. In adipocytes, it has been reported that SFAs stimulate pro-inflammatory responses through TLRs with JNK and NF-κB activation and block the insulin signaling cascade[53-55]. In accordance with previous data, SFA-challenged hypertrophic adipocytes increased pro-inflammatory responses (Fig. 4).

In this study, when adipocytes were chronically treated with free fatty acids for 6 days, the enlargement in fat cell size and the defect in insulin-dependent glucose uptake were similar in MUFA- and SFA-challenged hypertrophic adipocytes (Fig. 3, 6A, and 8). To rule out the potential involvement of SFA-induced inflammatory responses in the regulation of insulin sensitivity, MUFA-induced hypertrophic adipocytes were subjected to investigate the correlation between LD morphology and insulin sensitivity. I observed that insulin-dependent glucose uptake was less efficient in L/U-ADs than in S/M-ADs, S/U-ADs, and L/M-ADs. These results imply that impaired insulin sensitivity would be induced by excess lipid accumulation with enlarged LDs and cellular hypertrophy rather than inflammation.

Cortical actin assembly is essential for the maintenance of proper cell shape, motility, and many other cellular functions[56,57]. In adipocytes, cortical actin remodeling is associated with adipogenesis, triglyceride accumulation, LD formation, and GLUT4 trafficking[41,42]. In particular, it has been shown that

cortical actin assembly is involved in GLUT4-storage vesicle (GSV) docking and tethering to the plasma membrane, while microtubule organization is associated with the approach of GSVs[13]. GLUT4 is the major insulin-regulated glucose transporter; it coordinates insulin action in adipose tissue and muscle[58-60]. Adipose tissue-selective ablation of GLUT4 impairs insulin sensitivity in metabolic tissues, and adipose-selective overexpression of GLUT4 enhances glucose disposal and increases fat cell number (hyperplasia)[61,62]. Microarray analysis of primary adipocytes from mice fed short-term HFD showed that several cytoskeletal genes were upregulated or downregulated (Microarray data is available under GEO accession number GSE65557). Thus, given that adipocyte morphology is dramatically changed by cell size and/or LD locularity, it is plausible to speculate that cortical actin structures and/or microtubules that mediate GLUT4 translocation might be involved in adipocyte hypertrophy-induced insulin resistance. Here, I demonstrated that the amounts of GLUT4 translocated to the plasma membrane upon insulin clearly decreased in L/U-ADs (Fig. 10C). In addition, cortical actin structures were disrupted in L/U-ADs, indicating that decreased GLUT4 trafficking to the plasma membrane in L/U-ADs might be due to the disrupted cortical actin structure. However, I cannot exclude the possibility that disruption in the membrane fusion of GSVs, which can be modulated by SNAREs, also may contribute to impaired GLUT4 trafficking and insulin resistance in L/U-ADs.

TLR4 is a pattern-recognition receptor that plays a key role in the innate immune system by activating pro-inflammatory signaling pathways. C3H/HeJ mice which have a missense mutation in the third exon of the TLR4 gene have been widely used to investigate the role of TLR4 in the regulation of innate immunity[63,64]. Several TLR4 defective animal models exhibit different metabolic phenotypes in obesity, which are resulted from different HFD regime, animal sex, background strain, and various TLR4 mutations such as null and missense[65-69]. Nonetheless, most reports have consistently shown that C3H/HeJ mice are resistant to HFD-induced inflammation in adipose tissue. Here, to avoid complex circumstances in severe obesity and minimize the influences of immune cells, adipose tissues from short-term HFD fed mice with adipocyte hypertrophy were assessed for *ex vivo* study. Although C3H/HeJ mice were protective from pro-inflammatory responses upon short-term HFD, the degree of adipocyte hypertrophy and insulin resistance was similar to that of the control C3H/HeN mice (Fig. 12 and 13). These data indicate that adipocyte enlargement might be a crucial factor for inflammation independent insulin resistance *in vivo*.

Several lines of evidences support my idea that adipocyte hypertrophy is associated with insulin resistance *in vivo*, regardless of inflammation. First, in the case of Cushing's syndrome, patients with excess glucocorticoid develop central obesity and insulin resistance with suppressed immune responses. Second, the reduction of early B cell factor 1 (EBF1) increases adipocyte size

and provokes insulin resistance but does not influence the inflammatory pathways[33]. Third, my previous study shows that short-term HFD challenge in JNK1 knockout mice, Rag1 knockout mice (T-cell and B-cell depletion), and clodronate-treated mice (phagocytic macrophage depletion) induce adipocyte hypertrophy and insulin resistance independent of inflammatory responses[28].

In adipose tissue, adipocytes have parenchymal functions by having energy storage and energy release upon nutritional status. Unlike other cell types, adipocytes are able to buffer certain range of energy fluctuation for maintenance of whole body energy homeostasis. However, when chronic energy surplus overcomes buffering capacity of adipocytes, it appears that adipocyte would lose its parenchymal functions, resulting in insulin resistance as well as lipid dysregulation. In agreement with this idea, I showed that the changes of adipocyte size and LD morphology, which may represent the flexibility of adipocyte capacity, are closely associated with insulin resistance, probably, through cytoskeletal remodeling and GLUT4 trafficking. In adipocyte, it is likely that the nature of lipid metabolites would differentially affect the immune responses with different degree of inflammatory responses, while the characters of stored lipid metabolites would not affect adipocyte insulin resistance. I and others have proposed a provocative idea that initial adipose tissue immune response may participate in adipose tissue remodeling rather than insulin resistance to accommodate the changes of early obesity[28,45,70]. Instead, intense adipose tissue inflammation actively contributes to systemic

insulin resistance in severe obesity when the parenchymal functions of adipose tissue are rigorously impaired.

To date, most studies of adipose tissue insulin resistance have focused on investigating causal factors in prolonged or severe obesity. This approach may overlook the adipocyte-autonomous role in adipose tissue insulin resistance. For instance, it appears that adipose inflammation may reflect compensatory responses to a long-term imbalance in energy homeostasis. In this study, I demonstrated that adipocyte hypertrophy indeed induced insulin resistance, partly through impaired GLUT4 trafficking, concomitant with cortical actin disorganization (Fig. 16). In addition, I observed that adipocyte hypertrophy-induced insulin resistance appeared to be uncoupled from pro-inflammatory responses at the early stage of obesity. In conclusion, my data suggest that adipocyte hypertrophy *per se* would be a primary determinant of adipose tissue insulin resistance in early obesity, independent of inflammatory responses.

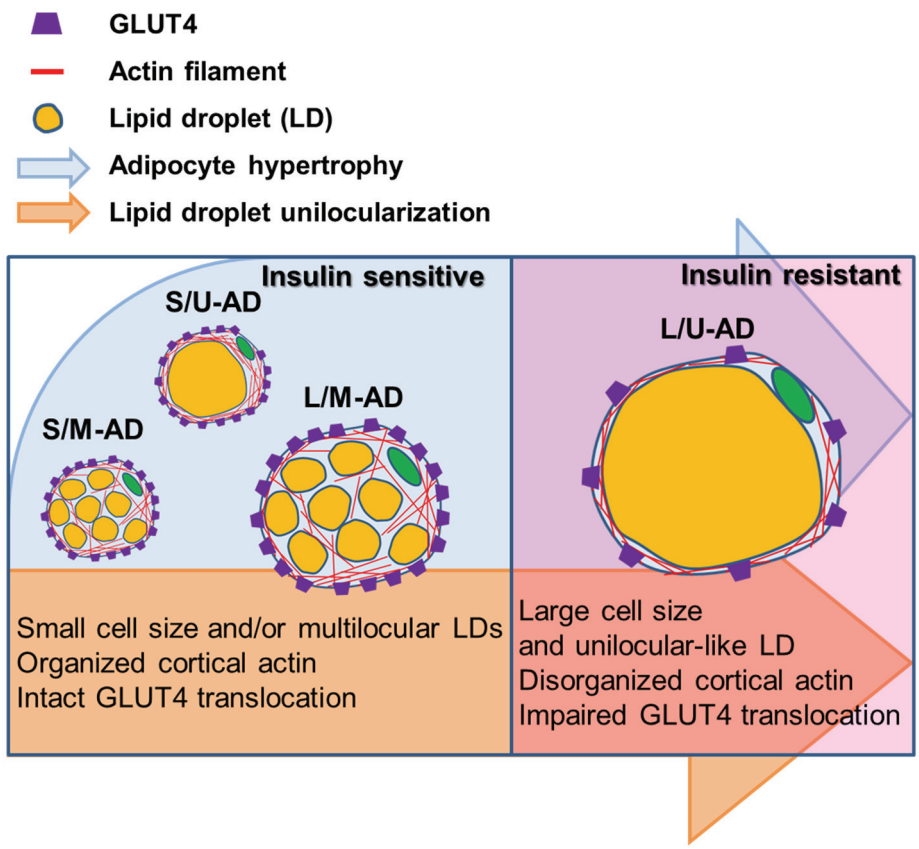

Figure 16. Graphical summary illustrating adipocyte hypertrophy-induced insulin resistance. Hypertrophied adipocytes with unilocular-like lipid droplets show decreased GLUT4 translocation to the plasma membrane and disorganized cortical actin structures. Hypertrophy-mediated impairment of GLUT4 translocation results in adipocyte insulin resistance regardless of inflammation.

CHAPTER TWO:

Adipocyte lipid droplets play a key role in regulating insulin-dependent glucose uptake via control of F/G-actin dynamics

ABSTRACT

Different adipocytes have unique traits in their morphologies and energy homeostasis according to their anatomical locations. However, it has not been thoroughly understood whether adipocytes with different lipid droplet shape could modulate insulin sensitivity. In this study, I demonstrate that adipocyte remodeling with different lipid droplet configuration plays an important role in insulin-dependent glucose uptake ability, accompanied with actin cytoskeleton dynamics. Compared to white adipocytes, brown/beige adipocytes with multilocular lipid droplets (LDs) exhibited relatively well-developed filamentous (F)-actin structure and potentiated glucose transporter 4 (GLUT4) translocation to plasma membrane upon insulin. On the contrary, LD enlargement and unilocularization in adipocytes downregulated the ratio of F/G-actin and subsequently suppressed insulin-dependent GLUT4 trafficking. Moreover, pharmacological inhibition of actin polymerization with impaired F/G-actin dynamics reduced glucose uptake in adipose tissue and conferred systemic insulin resistance in mice. Together, these results suggest that adipocyte remodeling with different LD configuration would be a crucial factor to determine insulin sensitivity by modulation of F/G-actin dynamics.

INTRODUCTION

White adipocytes primarily store excess energy sources in the form of neutral lipids while brown adipocytes dissipate them into heat. Also, beige adipocytes arise in subcutaneous adipose depot upon cold or β-adrenergic stimuli and exhibit morphological and functional changes like brown adipocytes[71-74]. Adipocytes from different fat depots show distinct morphological and functional traits. While white adipocytes usually contain a single (unilocular) lipid droplet (LD), brown/beige adipocytes contain numerous smaller (multilocular) LDs[75]. Recent studies have demonstrated that brown adipose tissue (BAT) absorbs higher levels of glucose than white adipose tissue (WAT) in response to basal and insulin stimulated states[76-80], which would be crucial for efficient thermogenesis in brown adipocytes. However, it remains elusive whether adipocyte morphology with different LD shapes might contribute to insulin-dependent glucose uptake ability in adipocytes.

Adipose tissue (AT) dynamically remodels its morphology and function upon environmental stimuli. For instance, in pathological condition such as obesity, unhealthy remodeling of AT accompanied with adipocyte hypertrophy, pro-inflammatory response, and hypoxia leads to insulin resistance. Also, in physiological condition such as thermoneutrality, BAT undergoes WAT-like remodeling and becomes prone to obesity-induced insulin resistance[81,82]. On the contrary, after cold exposure or physical exercise, white

adipocytes can acquire brown-like morphology and functions[73,74,83-85]. Moreover, it has been reported that formation of beige adipocytes in subcutaneous depot potentiates insulin-dependent glucose uptake in WATs and improves systemic insulin resistance[74,84-86]. Together, these findings imply that there might be certain relationships between adipocyte morphology with different LD configuration (size and locularity) and glucose uptake ability.

In adipocytes, glucose transporter 4 (GLUT4) is the major insulin-stimulated glucose transporter to uptake glucose. GLUT4 can travel along actin cytoskeleton as it is contained in GLUT4-storage vesicles (GSVs) [87-89]. During basal state, GLUT4 is mostly located in intracellular GSVs, trans-Golgi network, and recycling endosomes. On the other hand, GSVs quickly translocate to plasma membrane (PM) along actin cytoskeleton in the presence of insulin stimulation[13,87,90]. Upon insulin, Akt phosphorylates AS160, a Rab GTPase-activating protein, followed by Rab-mediated membrane trafficking of GSVs, eventually leading to uptake glucose[91-94]. It has been shown that genetic ablation of GLUT4 in whole body or adipose tissue impairs systemic glucose tolerance and insulin sensitivity[61,95]. On the contrary, overexpression of GLUT4 in whole body or adipose tissue improved glucose utilization in lean mice and ameliorated diabetic phenotype of *db/db* mice[96,97]. Thus, it has been suggested that adipose GLUT4 would be an essential player to regulate systemic insulin sensitivity. However, the underlying mechanisms of intracellular translocation of GLUT4 in adipocytes with different LD configurations under

pathophysiological conditions such as obesity or β-adrenergic stimuli are poorly understood.

Evolutionarily well conserved actin is the most abundant intracellular cytoskeletal protein that forms filamentous structures[30,31]. Actin exists as a globular monomer called G-actin and as a filamentous polymer called F-actin, which is a linear chain of G-actin subunits. The dynamics of intracellular G-actin and F-actin ratio is key property of actin remodeling. Actin is indispensable for numerous cellular functions including cell movement, intracellular vesicle transport, and maintenance of cell shape[98,99]. In adipocyte , it has been reported that actin remodeling plays a crucial role for the LD formation and morphological maturation during differentiation[100]. Also, a number of evidences of actin remodeling in the regulations of gene expression and insulin signaling have recently been revealed, suggesting the physiological significance of such regulation in adipocytes[101,102]. However, it is largely unknown which factors could modulate F/G-actin dynamics in adipocytes upon various circumstances.

While functional and morphological differences of white adipocytes and brown/beige adipocytes in the aspect of energy utilization and LD configuration have been well documented, the direct relationship between adipocyte functions and morphology are largely unknown. In this study, I have demonstrated that adipocyte remodeling with different LD configuration would

be a key factor and determine insulin sensitivity, accompanied with dynamic F/G-actin ratio. In the presence of physiological and pathological stimuli, I have investigated GLUT4 trafficking and glucose uptake abilities of adipocytes in different morphologies. Collectively, my data suggest that adipocyte remodeling with different LD size and locularity could determine insulin-dependent glucose uptake through the regulation of F/G-actin dynamics and GLUT4 trafficking.

MATERIALS AND METHODS

Animals

8-week-old male C57BL/6J and *db/+*, *db/db* mice were obtained from Central Lab Animal Inc. (Seoul, South Korea). All mice were maintained under specific pathogen-free conditions and were housed in solid-bottom cages with wood shavings for bedding in a room maintained at 25°C with a 12:12-hour light:dark cycle (lights on at 07:00). For thermoneutral and cold-exposure experiments, 8–10-week-old male mice were placed at 30°C for 7 days and then split into two groups: one group was exposed to thermoneutral condition and the other group to cold (4°C) for 6 days. For diet-induced obesity (DIO) experiment, after a stabilization period of at least 1 week, mice (8 weeks old) were fed a normal chow diet (NCD) until they were fed a 60% high fat diet (HFD) for the indicated times (Research Diets, Inc., NJ). The HFD mice were compared with age-matched chow-fed mice. The average initial body weights in each group of mice were not different. For the oral glucose tolerance test, the mice were fasted for 6 hours, basal blood samples were taken, and glucose was injected orally (2 g/kg). Blood samples were drawn at 15, 30, 45, 60, 90, and 120 minutes after injection. All animal procedures were in accordance with the research guidelines for the use of laboratory animals of Seoul National University.

Cell culture.

3T3-L1 preadipocytes were grown to confluence in Dulbecco's modified Eagle's medium (DMEM) supplemented with 10% bovine calf serum (BCS; Invitrogen Life Technologies, Carlsbad, CA). 2 days after the cells reached confluence (day 0), differentiation of the 3T3-L1 cells was induced in DMEM containing 10% fetal bovine serum (FBS; Invitrogen Life Technologies, Carlsbad, CA), methylisobutylxanthine (520 μM), dexamethasone (1 μM), and insulin (167 nM) for 48 hours. The culture medium was replaced on alternate days with DMEM containing 10% FBS and 167 nM insulin.

***In vitro/in vivo* imaging system**

3T3-L1 adipocytes were cultured on an 8-well chamber plate (Lab-Tek II). After differentiation, the cell culture medium was changed to a low-glucose medium (without FBS), and the cells were maintained in the new medium for 4 hours. The cells were then incubated for 1 hour in glucose-deficient DMEM (without FBS). For continuous monitoring of cellular glucose uptake with a DeltaVision imaging system (GE Healthcare), the 8-well chamber plate was loaded on the stage of the microscope. After pretreatment with 5 μm GB-Cy3 [36], 100 nM insulin was administered. Fluorescence images were recorded every 2 minutes. The images were digitized and saved on a computer for further analysis. The temperature of the chamber was maintained at 37°C.

Adipose tissues were removed and sliced into sections of 5 × 5 × 2 mm. Sliced samples were incubated in low-glucose DMEM containing 0.1% BSA for 30 minutes at 37°C. Sliced samples were incubated with 50 μM GB-Cy3 for 30 minutes in the presence or absence of 1 μM insulin. After several washes with PBS-Tween 20, the adipocytes were stained with fluorescein isothiocyanate-conjugated BODIPY. The samples were then stained with Vectashield solution (Vector Labs Inc.) containing 4′,6-diamidino-2-phenylindole (DAPI) and observed using a Zeiss LSM 700 confocal microscope (Carl Zeiss).

Mouse primary adipocytes isolation

Adipose tissue was fractionated as previously described, with minor modifications [103]. Briefly, eWAT were digested with type I collagenase buffer and filtered through nylon mesh. After centrifugation, the floating adipocytes and pelleted stromal vascular cell (SVC) fractions were washed several times and then collected for RNA extraction or imaging.

F/G-actin isolation and quantification

The tissues or cells used for F-actin/G-actin experiments were sonicated in a cold lysis buffer containing 10 mM K2HPO4, 100 mM NaF, 50 mM KCl, 2 mM MgCl2, 1 mM EGTA, 0.2 mM dithiothreitol (DTT), 0.5% Triton X-100, 1

mM sucrose (pH 7.0) and centrifuged at 15,000g for 30 min. The supernatant was collected to measure the soluble form of actin (G-actin). The pellet containing the insoluble form of actin (F-actin) was resuspended in lysis buffer plus an equal volume of a second buffer containing 1.5 mM guanidine hydrochloride, 1 mM sodium acetate, 1 mM CaCl2, 1 mM adenosine triphosphate, 20 mM tris-HCl (pH 7.5) and incubated on ice for 1 hour with gentle mixing every 15 min. The samples were centrifuged at 15,000 g for 30 min, and the supernatant containing F-actin was collected. Samples from the supernatant (G-actin) and pellet (F-actin) were loaded in equal amount and analyzed on Western blots.

Statistical analysis

Results represent data from multiple (three or more) independent experiments. Error bars represent standard deviation, and *P* values were calculated using Student's t-test or ANOVA.

Microarray data accession number. Microarray data are available under Gene Expression Omnibus (GEO) accession number GSE13432, GSE4899, GSE84860, and GSE8044. (http://www.ncbi.nlm.nih.gov/geo)

RESULTS

Warm and cold stimuli reversely regulate LD locularity and insulin-dependent glucose uptake in adipocytes

In inguinal WAT (iWAT), adipocytes can acquire brown-like phenotype and function upon cold exposure[74,84,104]. On the contrary, thermoneutral condition suppresses thermogenic program and induces white adipocyte-like morphology in BAT[82,105]. To test the morphological and functional changes of each fat depot upon different temperature stimuli, mice were exposed to thermoneutral (30°C) and cold temperature (4°C) conditions as well as room temperature. Consistent with previous reports[73], unilocular LD in white adipocytes was converted into multilocular LDs upon cold exposure while multilocular LDs in brown adipocytes became unilocular LD under thermoneutral condition (Fig. 17A). Moreover, I found that iWAT under cold condition upregulated insulin-dependent glucose uptake while BAT under thermoneutral condition remarkably downregulated insulin-dependent glucose uptake (Fig. 17B). Next, to examine whether the degree of insulin-dependent glucose uptake might be resulted from altered insulin signaling cascade, I assessed the phosphorylation events of insulin downstream signaling in each fat depot. As shown in Fig. 17C, there were no significant changes in insulin downstream cascades. To further affirm different insulin sensitivity in morphologically transformed adipocytes, I performed insulin-dependent Cy3

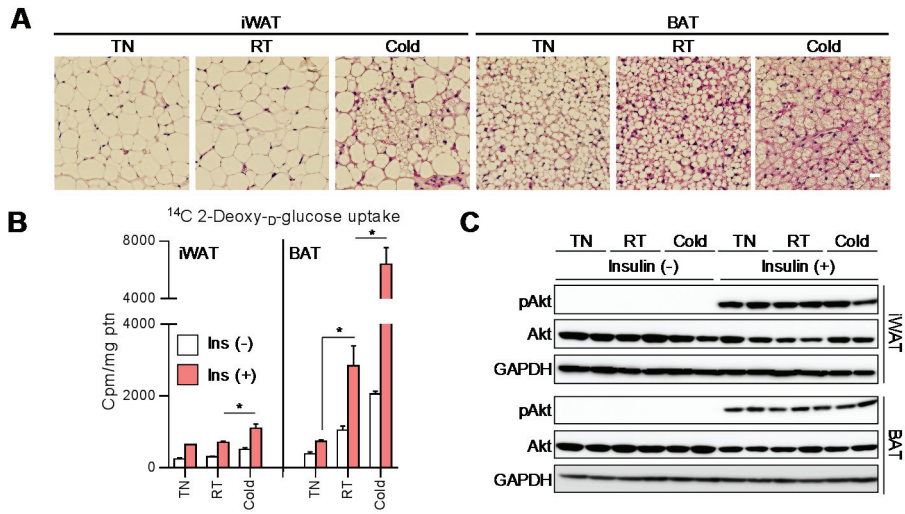

Figure 17. Changes in insulin-dependent glucose uptake of ATs from different temperature conditions. 8 week-old male C57B6L/J mice were placed in thermoneutral condition (30°C) for 1 week then were transferred to cold chamber (4°C) for another 1 week. (A) Adipocytes lipid droplet (LD) locularity were detected in inguinal white adipose tissue (iWAT) and brown adipose tissue (BAT) by hematoxylin and eosin (H&E) staining. (B) Insulin-dependent glucose uptake assays using [^{14}C]deoxyglucose. *, P< 0.05; **, P< 0.01. (C) Immunoblot analysis of iWAT and BAT. Phosphorylation of Akt (Ser308) with or without insulin (100 nM) treatment.

fluorescent-labeled glucose bioprobe (GB-Cy3) uptake assay[36,106,107]. Surprisingly, I discovered that in iWAT, cold exposure-induced multilocular adipocytes showed much higher extents of glucose absorption (Fig. 18; box 1 vs. 2). Furthermore, in BAT, thermoneutral condition-induced unilocularized brown adipocytes exhibited diminished insulin-dependent glucose uptake ability compared to multilocular brown adipocytes under room temperature condition (Fig. 18; box 3 and 4), which is consistent with quantitative analysis in isolated primary adipocytes (Fig. 17B). Together, it seems that these data provide a provocative idea that reversible transformation of adipocyte LD configuration might play a crucial role in the regulation of glucose uptake ability in adipocytes.

In adipocytes, transformation of LD locularity is associated with insulin-dependent glucose uptake ability

Adipocytes dynamically remodels their morphologies in the aspects of LD size and locularity upon various physiological and pathological conditions. To investigate whether reversible transformation of adipocyte morphology would dynamically modulate glucose uptake capacity, I decide to explorer cell culture model system that can switch unilocularization or multilocularization of LDs in adipocytes. In differentiated 3T3-L1 adipocytes, oleic acids (OA)-overloaded adipocytes (OA group) gradually increased the

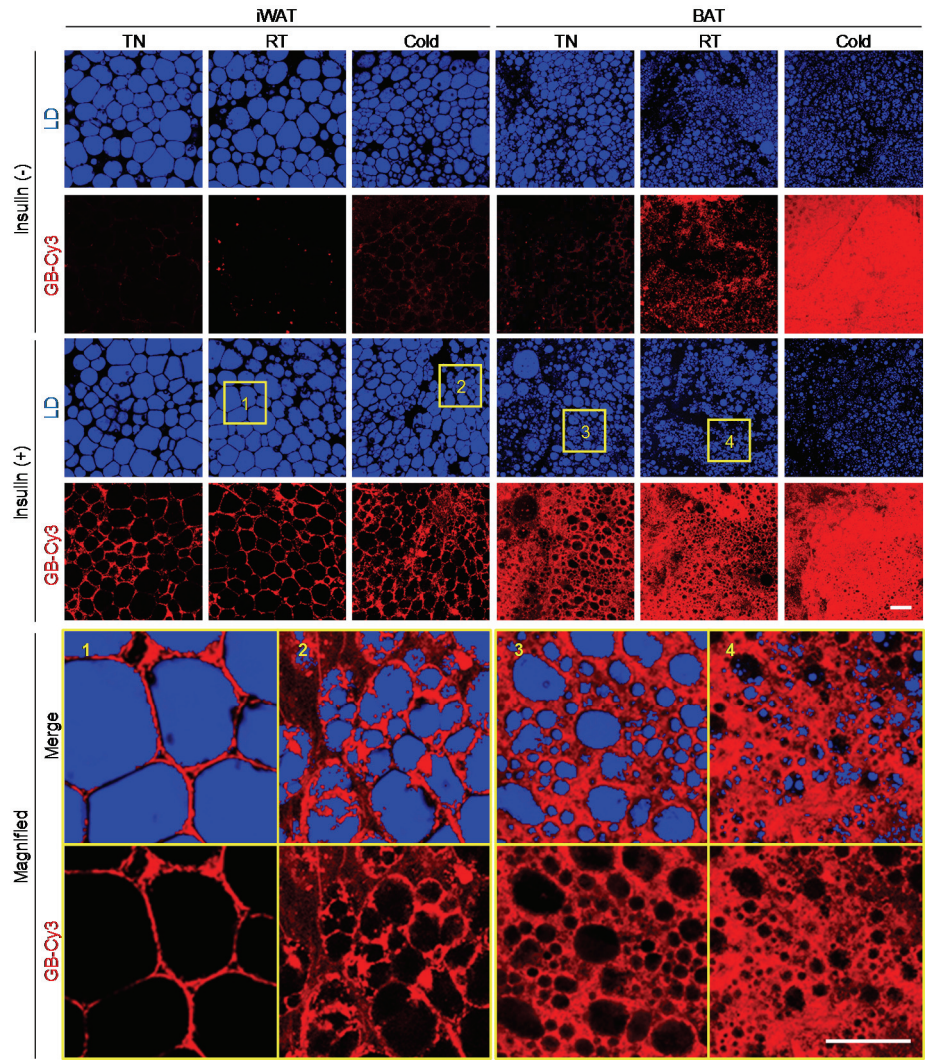

Figure 18. Changes in insulin sensitivity and adipocyte LD locularity of different temperatures. 8 week-old male C57B6L/J mice were placed in thermoneutral condition (30°C) for 1 week then were transferred to cold chamber (4°C) for another 1 week. *Ex vivo* glucose bioprobe uptake assay. iWATs and BATs from mice housed in different temperature conditions were ex vivo cultured with or without insulin (1 μM). Glucose bioprobe (GB-Cy3, 2 μM) was incubated for 30 min. Data presented are representative images.

volume of LDs and became unilocular adipocytes (Fig. 19A). On the other hand, subsequent treatment of β-adrenergic agonist, isoproterenol, in OA-overloaded adipocytes (OA+ISO group) reduced the volume of LDs and increased the number of LDs due to stimulated lipolysis (Fig. 19A). In accordance with above data (Fig. 17), adipocytes with a large unilocular LD in OA group showed decreased insulin-dependent glucose uptake ability while adipocytes with small multilocular LDs in OA+ISO group restored the ability of insulin-dependent glucose uptake (Fig. 19B) without significant changes in insulin downstream signaling (Fig. 19C). These results suggest that, in adipocytes, insulin-dependent glucose uptake ability would be reversibly regulated by LD size and locularity.

The ratio of F/G-actin dynamics is responsible for the control of insulin-dependent GLUT4 translocation in adipocytes with different LD locularity

Given that insulin downstream signaling was not altered by transformation of adipocyte morphology, the level of insulin-stimulated GLUT4 trafficking to PM was assessed in adipocytes with different LD configurations by using TIRF microscope. Upon insulin, differentiated 3T3-L1 adipocytes with multilocular LDs (CTL group) exhibited ~6-fold increase of GLUT4 signals in PM (Fig. 20A and B). On the contrary, adipocytes with unilocular large LD (OA group) severely downregulated insulin-dependent

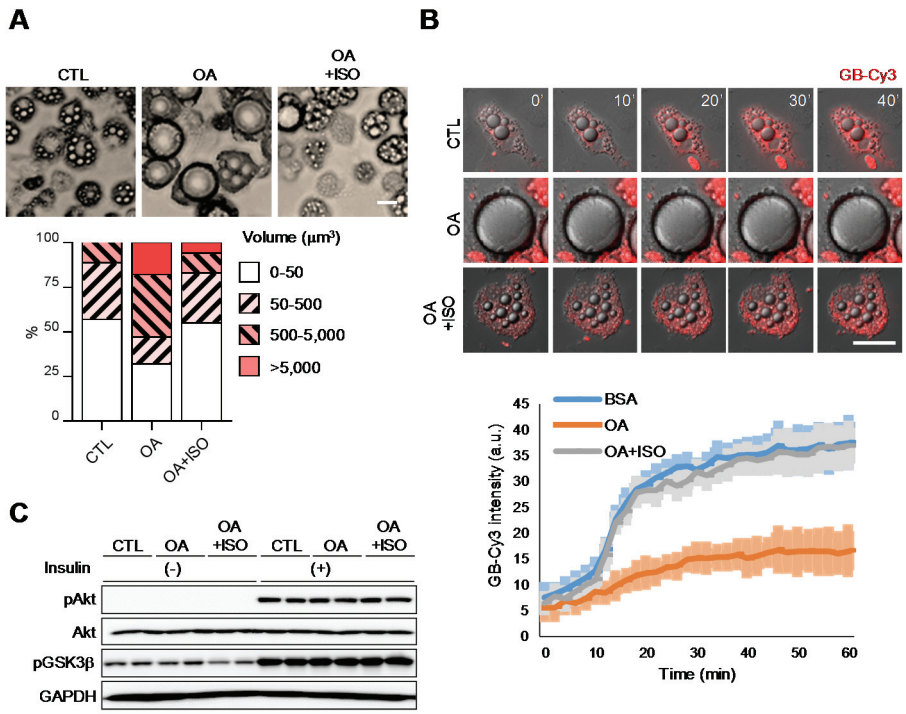

Figure 19. Reversible changes of LD locularity and insulin-dependent glucose uptake ability. 3T3-L1 adipocytes were differentiated and then cultured for 6 days with OA (500 μM) followed by ISO (2 μM, 12 hr) treatment. CTL, control (BSA); OA, oleic acid; and ISO, isoproterenol. (A) Microscopic images were obtained. (B) Insulin-dependent glucose bioprobe uptake assay. Cells were cultured with or without insulin (10 nM). Glucose bioprobe (GB-Cy3) was incubated for 1 hr. (C) Immunoblot analysis of iWAT and BAT. Phosphorylation of Akt (Ser308) and GSK3b with or without insulin (10 nM) treatment.

GLUT4 translocation to PM (Fig. 20A and 3B). In adipocytes, reversible transformation of unilocular LD to multilocular LD by inducing lipolysis (OA+ISO group) restored insulin-dependent translocation of GLUT4 to PM (Fig. 20A and B). Given that I have previously discovered that cortical F-actin is important to mediate translocation of GLUT4 to PM[107], I examined the degree of cortical F-actin structure in adipocytes with different LD configurations. As shown in Fig. 20C and D, cortical F-actin structure in adipocytes was reversibly modulated according to the LD configurations. OA-induced LD enlargement and unilocularization exerted ~50% reduction of cortical F-actin signal (Fig. 20C) while reacquisition of LD configuration similar to control adipocytes (OA+ISO group in Fig. 19A) restored cortical F-actin intensity to control level (Fig. 20A and C). Although adipocytes exhibited different degree of cortical F-actin upon LD configurations, total amounts of actin protein in adipocytes were not altered (Fig. 20E). As shown in Fig. 20E and 20F, transition of F-actin into G-actin was facilitated by LD unilocularization, resulting in reduced F/G-actin ratio, whereas LD multilocularization accelerated transition of G-actin into F-actin, to increase F/G-actin ratio. Thus, these data propose that reversible transformation of LD configuration in adipocytes would modulate GLUT4 trafficking and F/G-actin dynamics, eventually leading to determine insulin-dependent glucose uptake.

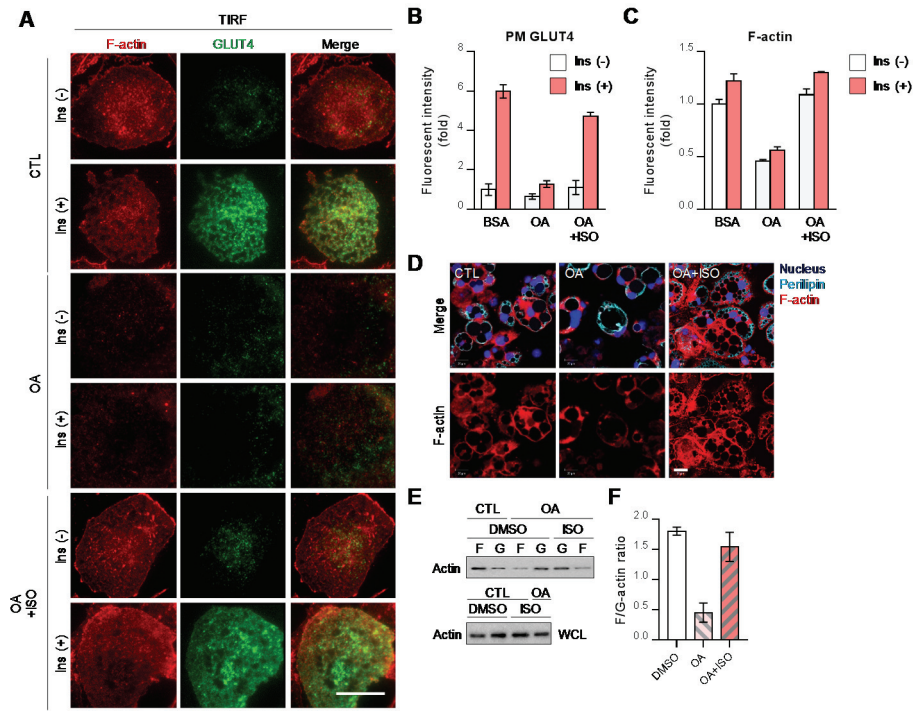

Figure 20. Reversible changes of insulin-stimulated GLUT4 trafficking in multi- or unilocular adipocytes. 3T3-L1 adipocytes stably expressing HA-GLUT4 were challenged with OA (500 μM) for 6 days followed by ISO (2 μM; 12 hr). The cells were fixed, stained with an anti-HA antibody and phalloidin-TRITC, and imaged on a total internal reflection fluorescence microscopy (TIRFM) in the presence or absence of insulin (100 nM). (A) Insulin-induced GLUT4 membrane insertion was examined by using TIRFM. Data presented are representative microscopic images of adipocyte in each indicated group. (B and C) TIRF intensities of each group were measured by using ImageJ. (E and F) Dynamic changes of F/G-actin ratios were quantified.

Thermoneutral condition-induced LD unilocularization in BAT downregulates insulin-dependent GLUT4 translocation

In contrast to unilocular white adipocytes, brown adipocytes contain innate multilocular LDs. However, under thermoneutral condition, multilocular brown adipocytes transformed into unilocular adipocytes. To test the relationship between reversible LD locularity and insulin-dependent GLUT4 trafficking ability in adipocytes, primary brown adipocytes were isolated from mice exposed under room temperature (RT group) or thermoneutral condition (TN group). Primary brown adipocytes from RT group showed multilocularity while primary brown adipocytes from TN group mostly exhibited unilocular (Fig. 21A). In TN group, the size of brown adipocytes became slightly but substantially increased, accompanied with unilocular LD (Fig. 21B). Consistent with the data from cell culture system, LD unilocularization in brown adipocytes showed the reduction in insulin-dependent GLUT4 translocation to PM (Fig. 21A and C). Moreover, F-actin structure and F/G-actin ratio were downregulated in BAT from TN group (Fig. 22A and B). In addition, upon cold exposure (Cold group), newly emerged multilocular beige adipocytes in iWAT exhibited elevated cortical F-actin structure (Fig. 22C) and upregulated F/G-actin ratio compared to unilocular white adipocytes in RT or TN group (Fig. 22D). Together, these *in vivo* data suggest that intrinsic differences of LD locularity and size in white and brown/beige adipocytes would be responsible for different capacity of insulin-dependent glucose uptake in adipocytes.

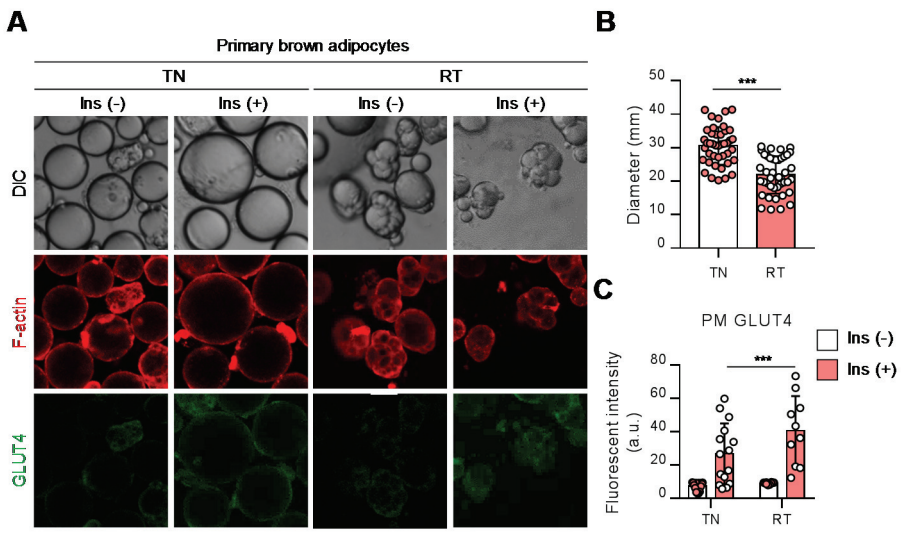

Figure 21. Higher insulin-dependent glucose uptake in multilocular brown adipocytes *in vivo*. Primary brown adipocytes were isolated from BAT of 8 week-old male C57B6L/J mice which were housed in RT or TN 1 week. (A) F-actin and plasma membrane anchored GLUT4 of primary cultured brown adipocytes were assessed by immuhistochemistry in the presence or absence of insulin (1 μM, 30 min). (B) Average diameters of isolated primary brown adipocytes. (C) Average intensities of plasma membrane anchored GLUT4 of isolated primary brown adipocytes.

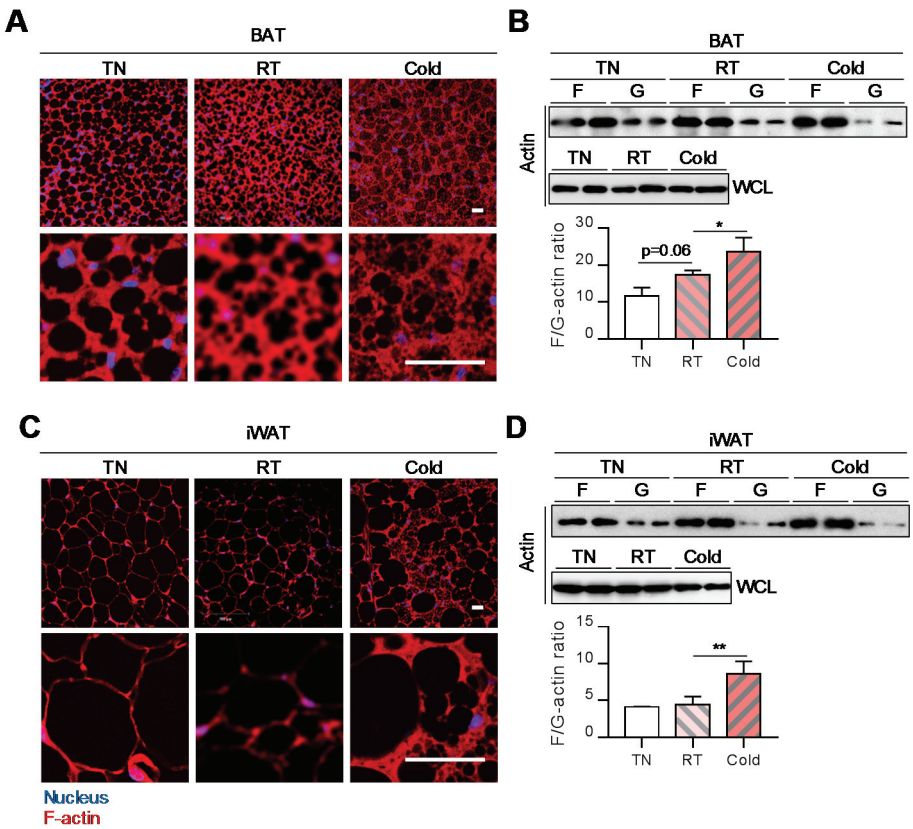

Figure 22. Dynamic changes of F/G-actin ratios in brown adipose tissues upon different temperature stimuli *in vivo*. 8 week-old male C57B6L/J mice were housed in TN, RT, or Cold for 1 week. (A) F-actin structures in BAT. (B) F/G-actin ratios in adipocytes from BAT were quantified. (C) F-actin structures in iWAT. (D) F/G-actin ratios in adipocytes from iWAT were quantified.

Obesity-induced LD enlargement in WAT suppresses insulin-dependent GLUT4 translocation

It has been previously reported that adipocyte hypertrophy *per se* could attenuate insulin-dependent glucose uptake in lipid-overloaded adipocytes[107]. Given that LD enlargement primarily decides adipocyte size, I have investigated whether LD expansion would affect insulin-dependent glucose uptake ability in primary white adipocytes. To tackle this, isolated primary white adipocytes were subjected to examine GLUT4 translocation to PM and cortical F-actin with or without insulin. After short-term high-fat diet (HFD) feeding (1 week), the sizes of primary white adipocytes were significantly increased (Fig. 23A and B). Next, to examine whether the size of unilocular LD in primary white adipocytes would affect cortical F-actin formation and GLUT4 trafficking ability, F-actin and PM GLUT4 were stained with fluorescent dye and antibody against an external epitope of GLUT4, respectively (Fig. 23C). Nonetheless, the degrees of PM GLUT4 and cortical F-actin fluorescent signals showed negative correlations upon adipocytes size (Fig. 23C and D). Compared to relatively small adipocytes, large adipocytes with their diameters over 100 μm exhibited enhanced negative correlation between fat cell size and PM GLUT4 (Fig. 23C; r=-0.28 → r=-0.81). Moreover, the negative correlations between F-actin fluorescent intensity and fat cell size were also increased in large adipocytes (> 100 μm) rather than small adipocytes

(< 100 μm) (Fig. 23D; r=-0.57 → r=-0.81). Along with the reduced PM GLUT4 and cortical F-actin signals in hypertrophic adipocytes, the ratio of F/G-actin cytoskeleton was significantly decreased in obese WAT (Fig. 23F and G). In accordance with the positive correlation between F-actin and PM GLUT4 (Fig. 23E; r=0.49), it is very likely that reduced PM GLUT4 and cortical F-actin in hypertrophic adipocytes would result in decreased insulin-dependent glucose uptake in obese WAT (Fig. 23H). These data propose that LD enlargement could deteriorate insulin-dependent glucose uptake in hypertrophic adipocytes via downregulation of F/G-actin ratio and GLUT4 translocation to PM.

Impairment of F-actin formation in adipose tissue induces systemic insulin resistance

To further elucidate the role of F/G-actin dynamics in the regulation of insulin-dependent glucose uptake ability in adipocytes, I examined insulin-dependent glucose uptake from *ex vivo* cultured WAT with or without cytochalasin D (CytD), an inhibitor of actin polymerization. In the presence of CytD, the formation of F-actin in WAT was greatly downregulated (Fig. 24A). Furthermore, the degree of insulin-dependent glucose uptake in *ex vivo* cultured WAT was markedly diminished by CytD (Fig. 24B). To examine the effects of F/G-actin dynamics on insulin sensitivity *in vivo*, CytD was administrated onto

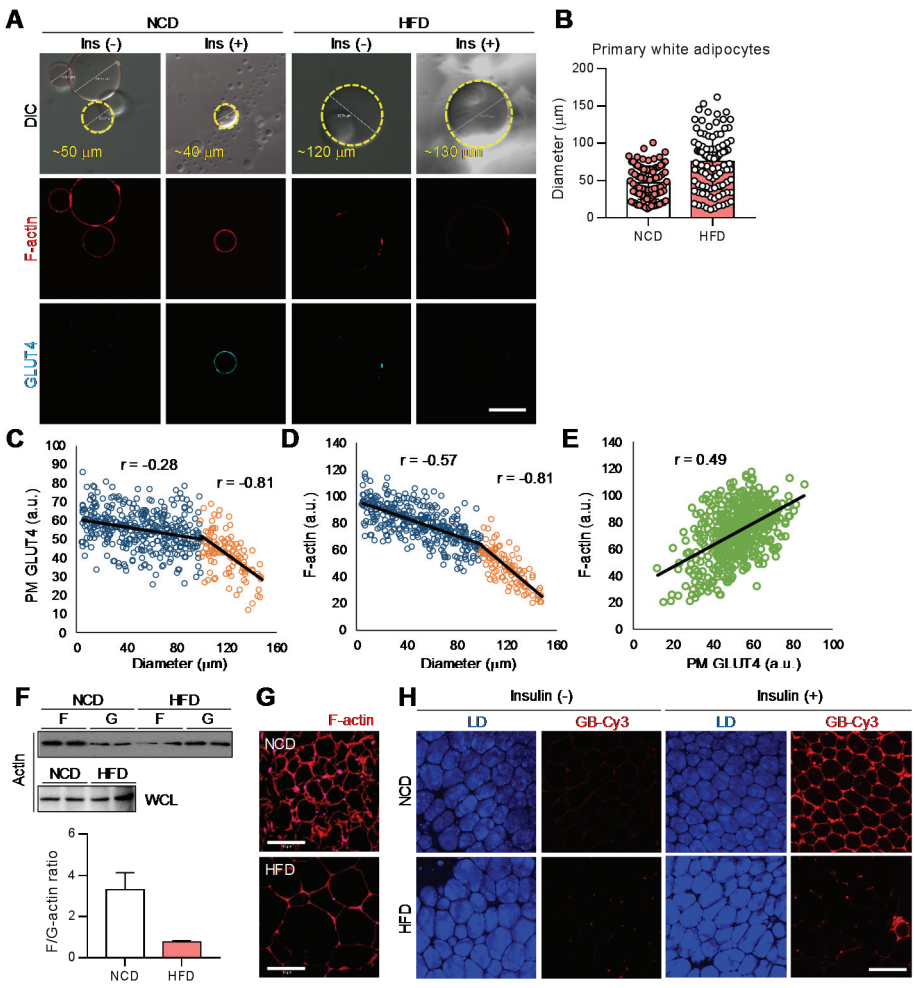

Figure 23. Impaired insulin-dependent GLUT4 translocation in hypertrophic adipocytes *in vivo*. Primary white adipocytes were isolated from eWAT of 8 week-old male C57B6L/J mice which were fed with HFD for 1 week. (A) F-actin and plasma membrane anchored GLUT4 of primary cultured white adipocytes were assessed by immuhistochemistry in the presence or absence of insulin (1 μM, 30 min). (B) Diameter of isolated primary white adipocytes were quantified. (C-E) Fluorescent intensities of plasma membrane anchored GLUT4 and F-actin. (F) F/G-actin ratios were quantified. (G) F-actin structures in eWAT of lean and obese mice. (H) *Ex vivo* glucose bioprobe uptake assay.

mice. As shown in Fig. 24C and D, CytD clearly decreased F-actin formation and reduced F/G-actin ratio in WAT. More importantly, CytD-treated mice exhibited glucose intolerance (Fig. 24E) and insulin intolerance (Fig. 24F). These *ex vivo* and *in vivo* data indicate that F/G-actin dynamics in adipocytes would play important roles in the regulation of systemic insulin sensitivity. CytD, the formation of F-actin in WAT was greatly downregulated (Fig. 24A). Furthermore, the degree of insulin-dependent glucose uptake in *ex vivo* cultured WAT was markedly diminished by CytD (Fig. 24B). To examine the effects of F/G-actin dynamics on insulin sensitivity *in vivo*, CytD was administrated onto mice. As shown in Fig. 24C and D, CytD clearly decreased F-actin formation and reduced F/G-actin ratio in WAT. More importantly, CytD-treated mice exhibited glucose intolerance (Fig. 24E) and insulin intolerance (Fig. 24F). These *ex vivo* and *in vivo* data indicate that F/G-actin dynamics in adipocytes would play important roles in the regulation of systemic insulin sensitivity.

Actin severing protein regulates insulin-dependent GLUT4 translocation

I found that insulin-dependent GLUT4 trafficking in adipocytes was closely associated with reversible changes in LD configuration and F/G-actin dynamics (Fig. 20). To elucidate the key modulator(s) for LD configuration in adipocytes, transcriptomic analysis was performed. Differentially expressed

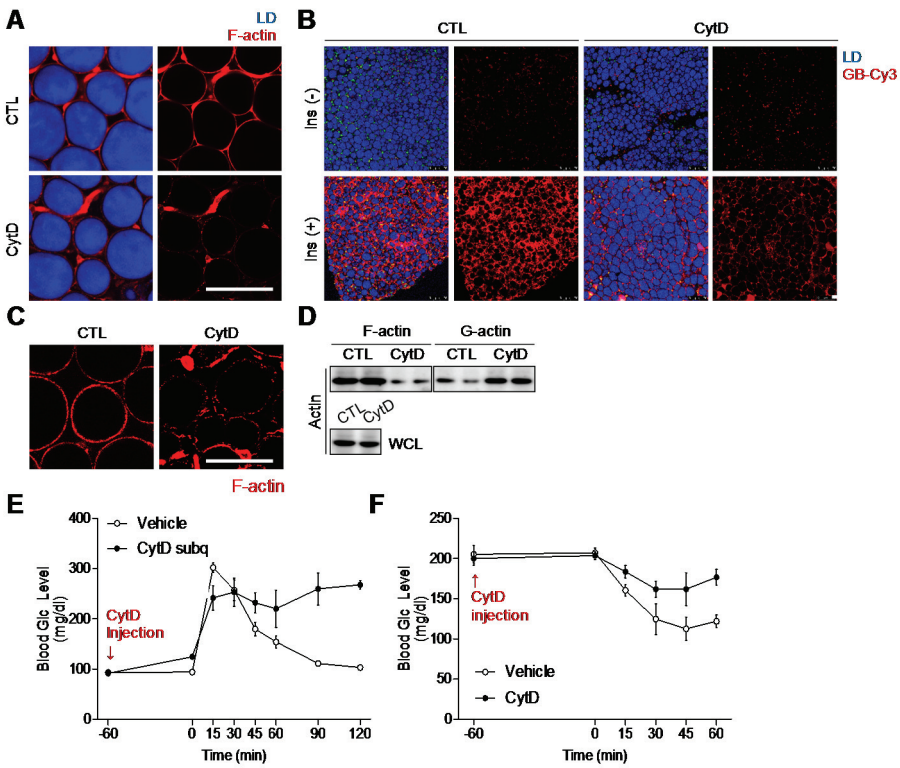

Figure 24. Systemic insulin resistance by F-actin disruption. *Ex vivo* cultured eWATs were treated with or without CytD (2 μM). (A) F-actin structures of eWAT. (B) Ex vivo insulin-dependent GB-Cy3 uptake assay. (C to F) CytD (200 nM/g) was administered to mice via intraperitoneal injection. (C) F-actin structures of eWAT. (D) The amount of F-actin and G-actin in eWAT. (E) Glucose tolerance test. (F) Insulin tolerance test.

genes (DEGs) and corresponding gene ontologies (GOs) from several transcriptomic datasets were analyzed by following criteria (Fig. 25A). As shown in Fig. 25B, actin binding GO (GO:0003779) was commonly downregulated in BAT compared to WAT, cold-stimulated WAT compared to TN control, and lean WAT compared to obese WAT (Table 2). Among DEGs in actin binding GO, several genes directly regulating F-actin elongation and severing were included (Fig. 25C; red). Among them, it is well known that activation Gelsolin and Cofilin1 promotes breakdown of F-actin (Table 3)[108]. Consistent with above transcriptomic analyses, the mRNA levels of Gelsolin and Cofilin1 were downregulated in BAT and iWATs under cold conditions (Fig. 25D). On the other hand, the mRNA and protein levels of Gelsolin and Cofilin1 were elevated in obese eWATs (Fig. 25E and F). Given that the actin severing activity of Cofilin1 is regulated by its phosphorylation status[109], I also examined the phosphorylation of Cofilin1 in WATs from lean and obese mice. As indicated in Fig. 25E, the levels of inhibitory phosphorylation of cofilin1 were relatively decreased in obese eWAT.

Next, to investigate the role of actin severing activity in the regulation of GLUT4 trafficking in adipocytes, I decided to overexpress gelsolin in differentiated 3T3-L1 adipocytes. Previously, it has been reported that ectopic overexpression of Gelsolin but not Cofilin1 markedly accelerates F-actin disassembly110. The reason why Gelsolin has more potent effect on F-actin could be, partly, explained by its higher affinity (picomolar Kd) for F-actin, as

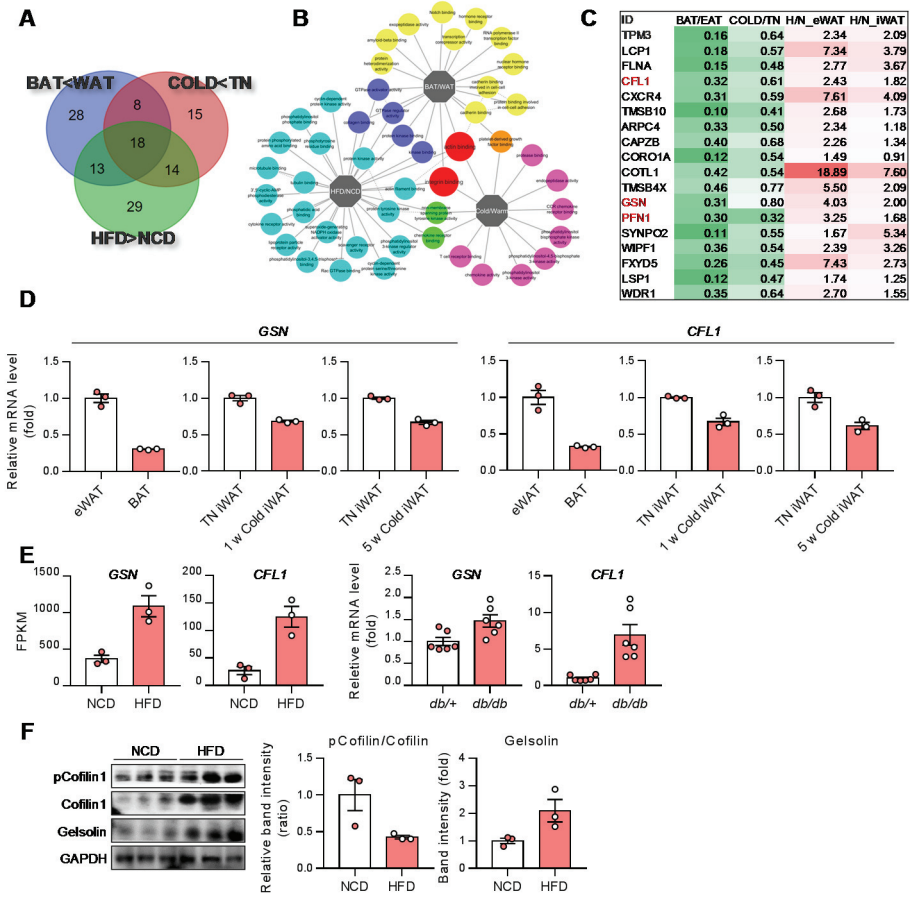

Figure 25. Elevation of actin severing genes in unilocular and enlarged adipocytes. Gene ontologies were analyzed from microarray and RNA-sequencing data. (A) Number of actin binding genes from indicated group. (B) Network of screened gene ontologies from each group. (C) Fold of changes of screened genes. (D and E) Relative mRNA levels of actin severing genes in indicated tissues. (F) Protein levels of Cofilin1 and Gelsolin in eWAT.

BAT>EAT 2-fold

Index	Name	P-value	Adjusted p-value	Z-score	Combined score
1	enoyl-CoA hydratase activity (GO:0004300)	0.00001893	0.003444	-2.97	32.33
2	acetyl-CoA C-acyltransferase activity (GO:0003988)	0.0001235	0.01124	-2.98	26.82
3	NADH dehydrogenase activity (GO:0003954)	0.0001063	0.01124	-2.71	24.78
4	NADH dehydrogenase (ubiquinone) activity (GO:0008137)	3.24E-07	0.00008848	-1.66	24.77
5	ubiquinone binding (GO:0048039)	0.0001235	0.01124	-2.58	23.25
6	NADH dehydrogenase (quinone) activity (GO:0050136)	3.24E-07	0.00008848	-1.56	23.24
7	3',5'-cyclic-nucleotide phosphodiesterase activity (GO:0004114)	0.0002359	0.0184	-2.28	19.06
8	long-chain fatty acid binding (GO:0036041)	0.002704	0.1476	-3.02	17.86
9	oxidoreductase activity, acting on diphenols and related substances as donors, cytochrome as acceptor (GO:0016681)	0.006068	0.2001	-3.48	17.78
10	ubiquinol-cytochrome-c reductase activity (GO:0008121)	0.006068	0.2001	-3.45	17.6

BAT<EAT 2-fold

Index	Name	P-value	Adjusted p-value	Z-score	Combined score
1	cadherin binding (GO:0045296)	6.74E-15	3.23E-12	-2.04	66.54
2	integrin binding (GO:0005178)	3.39E-15	3.23E-12	-1.45	48.39
3	actin binding (GO:0003779) *67 genes	0.000002516	0.0006031	-2.41	31.06
4	collagen binding (GO:0005518)	1.76E-10	5.63E-08	-1.33	29.83
5	cadherin binding involved in cell-cell adhesion (GO:0098641)	0.000005369	0.0008581	-2.07	25.18
6	platelet-derived growth factor binding (GO:0048407)	0.00007574	0.007287	-2.64	25.09
7	CD4 receptor binding (GO:0042609)	0.001267	0.05524	-3.69	24.64
8	phospholipid scramblase activity (GO:0017128)	0.01245	0.2251	-5.14	22.53
9	protein binding involved in cell-cell adhesion (GO:0098632)	0.00002048	0.002806	-2.02	21.85
10	exopeptidase activity (GO:0008238)	0.000003827	0.000734	-1.69	21.1

Cold 3 d>TN 2-fold

Index	Name	P-value	Adjusted p-value	Z-score	Combined score
1	NADH dehydrogenase (ubiquinone) activity (GO:0008137)	9.54E-15	2.21E-12	-1.66	53.51
2	NADH dehydrogenase (quinone) activity (GO:0050136)	9.54E-15	2.21E-12	-1.56	50.22
3	proton-transporting ATP synthase activity, rotational mechanism (GO:0046933)	0.009366	0.2	-6.41	29.96
4	telethonin binding (GO:0031433)	0.0001295	0.01498	-3.13	28
5	ubiquinone binding (GO:0048039)	0.00006674	0.0103	-2.6	25.04
6	long-chain fatty acid binding (GO:0036041)	0.001719	0.1137	-3.03	19.31
7	muscle alpha-actinin binding (GO:0051371)	0.0003345	0.03098	-2.4	19.17
8	acetyl-CoA C-acyltransferase activity (GO:0003988)	0.001719	0.1137	-2.97	18.94
9	phosphofructokinase activity (GO:0008443)	0.002672	0.1237	-3.05	18.07
10	enoyl-CoA hydratase activity (GO:0004300)	0.003895	0.1503	-2.92	16.21

Cold 3 d<TN 2-fold

Index	Name	P-value	Adjusted p-value	Z-score	Combined score
1	platelet-derived growth factor binding (GO:0048407)	0.00001304	0.003196	-2.68	30.11
2	T cell receptor binding (GO:0042608)	0.00002224	0.003196	-2.47	26.44
3	phosphatidylinositol-4,5-bisphosphate 3-kinase activity (GO:0046934)	0.00002678	0.003196	-1.85	19.45
4	actin binding (GO:0003779) *18 genes	0.0004535	0.01804	-2.36	18.18
5	CD4 receptor binding (GO:0042609)	0.0158	0.2356	-3.69	15.31
6	non-membrane spanning protein tyrosine kinase activity (GO:0004715)	0.0002406	0.01231	-1.72	14.33
7	phosphatidylinositol 3-kinase activity (GO:0035004)	0.00007033	0.005036	-1.46	13.99
8	phospholipase activator activity (GO:0016004)	0.0158	0.2356	-3.26	13.52
9	integrin binding (GO:0005178)	0.00008998	0.005369	-1.43	13.35
10	chemokine activity (GO:0008009)	0.0003666	0.0164	-1.69	13.34

Cold 5 w>TN 2-fold

Index	Name	P-value	Adjusted p-value	Z-score	Combined score
1	NADH dehydrogenase (ubiquinone) activity (GO:0008137)	1.34E-15	5.80E-13	-1.66	56.76
2	NADH dehydrogenase (quinone) activity (GO:0050136)	1.34E-15	5.80E-13	-1.56	53.27
3	NADH dehydrogenase activity (GO:0003954)	0.00001533	0.002652	-2.7	29.97
4	proton-transporting ATP synthase activity, rotational mechanism (GO:0046933)	0.0102	0.3393	-6.33	29.01
5	enoyl-CoA hydratase activity (GO:0004300)	0.000199	0.01565	-2.93	24.94
6	4 iron, 4 sulfur cluster binding (GO:0051539)	0.0001814	0.01565	-2.72	23.42
7	acetyl-CoA C-acyltransferase activity (GO:0003988)	0.0004585	0.03051	-2.94	22.61
8	3-hydroxyacyl-CoA dehydrogenase activity (GO:0003857)	0.000199	0.01565	-2.65	22.55
9	2 iron, 2 sulfur cluster binding (GO:0051537)	0.0001814	0.01565	-2.54	21.86
10	acyl-CoA dehydrogenase activity (GO:0003995)	0.00003034	0.004373	-2.09	21.74

Cold 5 w<TN 2-fold

Index	Name	P-value	Adjusted p-value	Z-score	Combined score
1	cadherin binding (GO:0045296)	9.10E-07	0.0002012	-2.03	28.25
2	kinase binding (GO:0019900)	4.37E-07	0.0001933	-1.58	23.19
3	actin binding (GO:0003779) * 50 genes	0.00006967	0.008798	-2.38	22.79
4	CD4 receptor binding (GO:0042609)	0.004299	0.1605	-3.7	20.15
5	dolichyl-diphosphooligosaccharide-protein glycotransferase activity (GO:0004579)	0.002838	0.1605	-3.27	19.16
6	RNA binding (GO:0003723)	9.10E-07	0.0002012	-1.36	18.87
7	cysteine-type endopeptidase activity (GO:0004197)	0.000007859	0.00139	-1.6	18.83
8	actin filament binding (GO:0051015)	0.00002899	0.004271	-1.75	18.31
9	protein kinase binding (GO:0019901)	3.00E-07	0.0001933	-1.11	16.65
10	transforming growth factor beta-activated receptor activity (GO:0005024)	0.004299	0.1605	-2.94	16.04

HFD>NCD 2-fold

Index	Name	P-value	Adjusted p-value	Z-score	Combined score
1	actin binding (GO:0003779) *74 genes	9.81E-20	8.46E-17	-2.44	106.7
2	actin filament binding (GO:0051015) *41 genes	4.11E-13	1.77E-10	-1.77	50.61
3	non-membrane spanning protein tyrosine kinase activity (GO:0004715)	3.99E-11	6.87E-09	-1.73	41.36
4	platelet-derived growth factor binding (GO:0048407)	0.0000018	0.00009125	-2.61	34.56
5	phosphotyrosine residue binding (GO:0001784)	1.06E-07	0.000007602	-2.01	32.21
6	integrin binding (GO:0005178)	8.31E-10	1.19E-07	-1.43	29.97
7	cadherin binding (GO:0045296)	2.14E-07	0.0000142	-1.95	29.91
8	protein kinase activity (GO:0004672)	2.18E-12	6.27E-10	-1.09	29.24
9	GTPase activator activity (GO:0005096)	2.98E-07	0.00001836	-1.94	29.13
10	protein phosphorylated amino acid binding (GO:0045309)	0.000001084	0.00005842	-2.08	28.54

HFD<NCD 2-fold

Index	Name	P-value	Adjusted p-value	Z-score	Combined score
1	glutathione transferase activity (GO:0004364)	2.94E-10	2.18E-07	-1.98	43.47
2	enoyl-CoA hydratase activity (GO:0004300)	0.002016	0.1492	-2.93	18.2
3	transcription factor activity, RNA polymerase II core promoter proximal region sequence-specific binding (GO:0000982)	0.00001626	0.006016	-1.62	17.88
4	transcriptional activator activity, RNA polymerase II core promoter proximal region sequence-specific binding (GO:0001077)	0.000145	0.02682	-1.92	17.01
5	RNA polymerase II regulatory region sequence-specific DNA binding (GO:0000977)	0.0001171	0.02682	-1.85	16.73
6	RNA polymerase II transcription factor activity, sequence-specific transcription regulatory region DNA binding (GO:0001133)	0.001635	0.1345	-2.34	15.03
7	protein homodimerization activity (GO:0042803)	0.001208	0.1117	-2.15	14.43
8	neurotrophin binding (GO:0043121)	0.02608	0.5948	-3.78	13.79
9	insulin-like growth factor receptor binding (GO:0005159)	0.003315	0.223	-2.33	13.32
10	oxidoreductase activity, acting on the CH-OH group of donors, NAD or NADP as acceptor (GO:0016616)	0.0009018	0.1023	-1.78	12.46

Table 2. Gene ontology analysis by EnrichR. DEGs form BAT/WAT, 3 d Cold/TN, 5 w Cold/TN, and HFD/NCD WATs were cross analyzed.

ID	BAT>WAT	Cold>TN 3 D	Cold>TN 5 W	HFD>NCD eWAT	HFD>NCD iWAT
TMSB10	0.096139033	0.555552479	0.606095427	6.394107783	2.719025799
CORO1A	0.118795895	0.846830063	0.289867474	7.98620521	2.382952377
FLNA	0.146012221	0.604783128	0.475622333	2.774836968	3.671235901
TPM3	0.162415534	0.581079961	0.637422148	2.33614064	2.093766147
LCP1	0.177099013	0.458791166	0.565493548	17.03012159	10.47969371
MYO1E	0.196662989	0.744729669	0.706779762	14.96464089	4.959545892
CCR5	0.218876484	0.43764949	0.765419092	5.870904694	3.162055763
FXYD5	0.258641659	0.529012511	0.447205392	8.351877105	2.750959156
GSN	0.305392386	0.80723113	0.802059887	4.034148141	2.002212686
CXCR4	0.310404127	0.8063109	0.585684031	7.613433152	4.091137729
MYO1F	0.319834248	0.627800089	0.517417136	21.42385065	9.516588457
CFL1	0.324474692	0.668110759	0.610747631	2.432074395	1.819279339
WIPF1	0.363623	0.540638777	0.548442236	2.387942465	3.26461755
COTL1	0.415846959	0.354667075	0.585713818	18.89075805	7.599142175
MYO9B	0.41776013	0.611083576	0.875769067	3.295817268	1.998625356
TMSB4X	0.459035921	0.813464498	0.769867935	5.498937947	2.091716418
ACTR3	0.503057097	0.644008762	0.72226417	5.237371697	2.720960903
WAS	0.536431708	0.39130368	0.652039657	7.459440219	2.62313287
ABL2	0.619027165	0.74166707	0.832778145	2.810607034	2.394624198

Table 3. Gene expression profiles of 19-screened genes in GO:0003779 "actin binding"

compared with Cofilin1 (micromolar K_d)[108,110]. Transient overexpression of gelsolin led to decreased F/G-actin ratio in adipocytes (Fig. 26A and B). In adipocytes, gelsolin-overexpression or CytD treatment-induced downregulation of F/G-actin ratio did not affect insulin signaling cascade (Fig. 26C). Nonetheless, insulin-dependent GLUT4 translocation to PM and glucose uptake ability were significantly attenuated by gelsolin overexpression (Fig. 26D and E). Together, these data implicate in the potential roles of F/G-actin dynamics, which is closely associated with LD locularity, in the regulation of insulin-dependent GLUT4 trafficking in adipocytes.

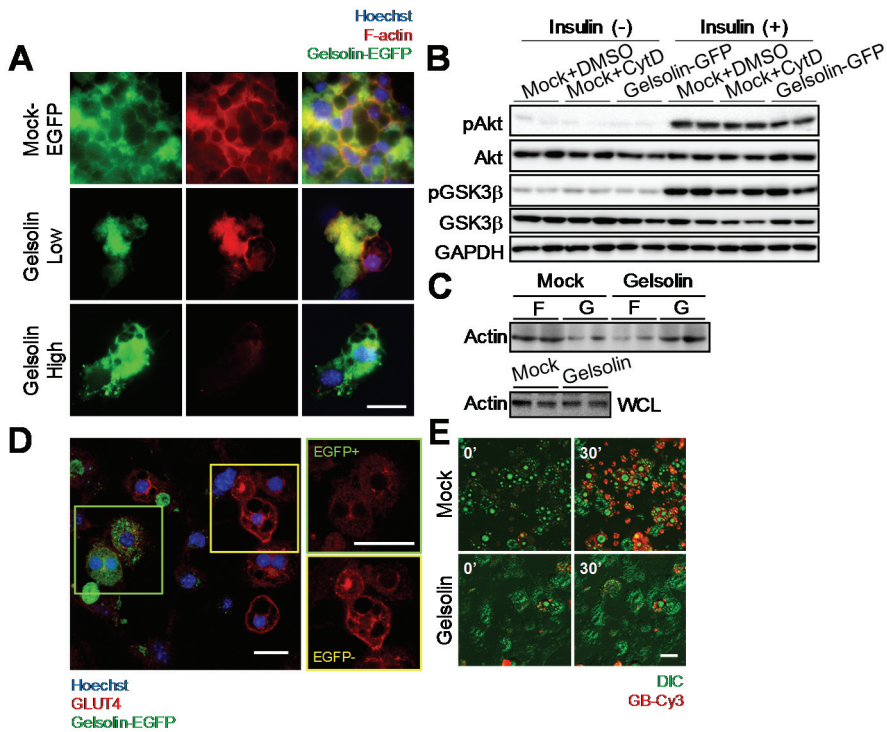

Figure 26. Gelsolin overexpression in adipocytes impairs F/G-actin dynamics. EGFP-Gelsolin was transfected to fully differentiated 3T3-L1 adipocytes. (A) F-actin structure of EGFP-Gelsolin-overexpressing adipocytes. (B) Immunoblot analysis of Gelsolin-overexpressed adipocytes. Phosphorylation of Akt (Ser308) and GSK3b with or without insulin (100 nM) treatment. (C) Changes of F/G-actin ratio by Gelsolin overexpression. (D) Impaired GLUT4 translocation to plasma membrane in Gelsolin-expressing adipocytes. (E) Insulin-dependent GB-Cy3 uptake assay.

DISCUSSION

Adipocytes are flexible and morphologically dynamic upon nutritional states. For energy homeostasis, adipocytes can efficiently uptake circulating glucose through GLUT4 in response to insulin[111]. However, it is not fully understood whether adipocyte morphology with different LD configurations would affect the degree of insulin-dependent glucose uptake ability. In this study, a number of evidences of relationship between LD configuration and GLUT4 trafficking ability have been observed, and the physiological significance of such association is becoming clear. For instance, LD multilocularization increased the insulin-dependent GLUT4 translocation while LD enlargement and/or unilocularization decreased GLUT4 trafficking even in the presence of insulin. In those processes, F/G-actin ratio was dynamically altered upon transformation of LD configuration, suggesting that actin cytoskeletal remodeling could mediate cell morphology and glucose uptake ability in adipocytes. Furthermore, genetic or pharmacological downregulation of adipocyte F/G-actin ratio resulted in impaired glucose uptake *in vitro* and *in vivo*. Therefore, my data provide novel concept that adipocyte LD configuration would be an important factor to control insulin sensitivity.

Adipocyte morphology considerably varies depending on anatomical locations and stimuli. Microscopically, LD configuration, the size and number

of LD, make easy to distinguish different adipocyte morphologies such as unilocular white adipocytes and multilocular brown/beige adipocytes. Here, I found that reversible conversion of unilocular LD into multilocular LDs in adipocytes potentiated insulin-dependent glucose uptake, implying that there might be a close association between LD configuration and insulin sensitivity in adipocytes. Considering that LD occupies most cytoplasmic portion in adipocyte, it is plausible to speculate that LD multilocularization or size reduction would provide increased cytoplasmic space to absorb more energy sources such as glucose. In an agreement with above conjecture, the fluorescence signals of glucose bioprobe (GB-Cy3) absorbed in multilocular adipocytes were enhanced in throughout the cytoplasm. On the other hand, the signals of absorbed GB-Cy3 in unilocular adipocytes were detected in the form of rim between PM and LD (Fig. 18 and 19B). These results imply that adipocyte LD configuration including size and locularity would be a key factor to decide the storage capacity in adipocytes.

Recently, it has been reported that insulin-dependent glucose uptake ability of brown adipocytes is significantly higher than that of white adipocytes even though the levels of GLUT4 protein in brown and white adipocytes are comparable at room temperature[78,112,113]. In this regard as well as the potential roles of LD configuration in the regulation of glucose storage capacity, it is feasible to hypothesize the idea that LD configuration might be associated with insulin-dependent GLUT4 trafficking in adipocytes. This idea was proven with

following *in vivo* and *ex vivo* data. As shown in Fig. 21A, thermoneutrality-induced LD unilocularization in brown adipocytes reduced insulin-dependent GLUT4 trafficking to PM. Reversely, β-adrenergic agonist-induced multilocularization in 3T3-L1 adipocytes (Fig. 19A, 20A, and B) or cold-induced multilocularization in white adipocytes (Fig. 27) exhibited elevated insulin-stimulated GLUT4 trafficking without significant changes in the total amounts of GLUT4 protein. These *in vivo* and *in vitro* findings implied a close relationship between LD locularity and insulin-dependent GSVs trafficking ability. Thus, it is plausible to speculate that intrinsic differences in LD locularity between white and brown/beige adipocytes might be a key factor to modulate insulin-dependent GLUT4 trafficking.

In adipocytes, activation of PI3K-Akt axis stimulates GLUT4 translocation to PM and cytoskeleton plays an important role as a molecular railroad for GSVs in this process[13,92]. Recent study has demonstrated that acute (4 hours) cold exposure or CL316,243 treatment promotes glucose uptake and phosphorylation of Akt in WAT and BAT, partly, due to acute increase of plasma insulin level[79]. In this study, I found that in cold-induced white adipocytes with multilocular LDs, insulin-dependent glucose uptake was markedly elevated without significant alterations of insulin signaling (Fig. 17). Thus, it seems that there might be another mechanism that potentially bypasses canonical insulin signaling to modulate insulin-dependent glucose uptake in adipocytes. Given that not only insulin signaling pathway but also actin

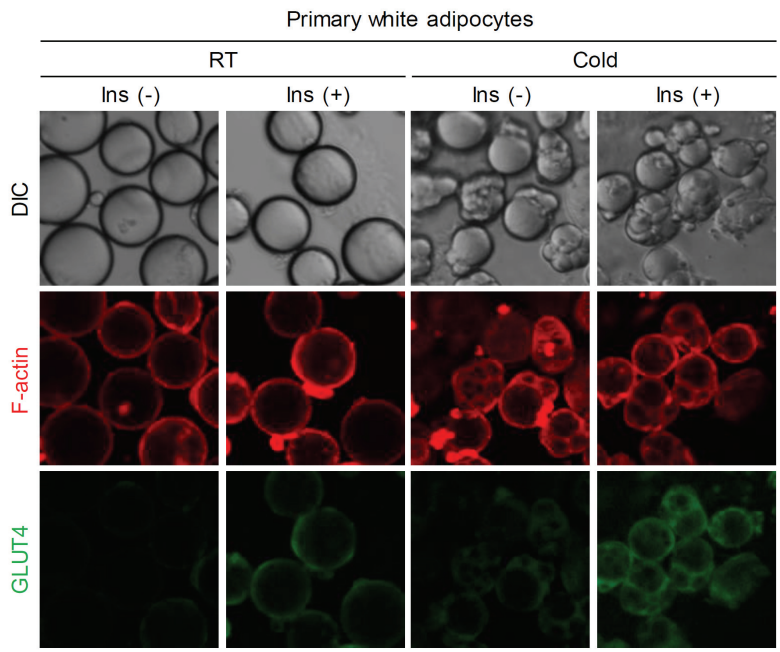

Figure 27. Higher insulin-dependent glucose uptake in multilocular beige adipocytes *in vivo*. Primary white adipocytes were isolated from iWAT of 8 week-old male C57B6L/J mice which were housed in RT or Cold 1 week. (A) F-actin and plasma membrane anchored GLUT4 of primary cultured white adipocytes were assessed by immuhistochemistry in the presence or absence of insulin (1 μM, 30 min).

cytoskeleton are indispensable for insulin-dependent GSVs trafficking in adipocytes[13,107,114], I examined actin dynamics in adipocytes with different LD configuration. Chemical inhibition of actin polymerization with CytD downregulated the ratio of F/G-actin and decreased insulin-dependent glucose uptake in adipocytes (Fig. 24). Furthermore, reduction of F/G-actin ratio by overexpression of gelsolin, an actin-severing enzyme, showed impaired insulin-dependent GLUT4 trafficking and glucose uptake in adipocytes (Fig. 26). Hence, my data propose that F/G-actin dynamics would be an important factor to regulate insulin-stimulated GSVs trafficking in adipocytes, which might be independent of canonical insulin signaling.

Here, I observed that insulin-dependent glucose uptake ability of adipocytes seemed to be closely related with LD configuration and F/G-actin ratio rather than insulin downstream signaling cascade, which might, partly, explained by the kinetics of GSVs and cytoskeletal tracks. Theoretically, if there is no difference in the signal for trafficking of the GSVs, the more the route, the more movement would be possible. In accordance with this assumption, multilocular adipocytes exhibited higher glucose uptake ability accompanied with potentiated insulin-stimulated GSVs trafficking than unilocular adipocytes, despite of no differences in insulin signals (Fig. 19 and 20). More importantly, I observed that the level of insulin-stimulated PM localized GLUT4 showed strong positive correlation with cortical F-actin by analyzing primary adipocytes from lean and obese ATs (Fig. 23). Thus, these

findings indicate that actin cytoskeleton would not only be a precondition for GLUT4 trafficking ability but also its remodeling could actively modulate insulin-dependent GLUT4 translocation in adipocytes according to LD morphology.

From the transcriptome analyses, actin-severing genes such as Gelsolin and Cofilin1 were upregulated in HFD-induced hypertrophic adipocytes but downregulated in brown/beige adipocytes. Considering the enzymatic activity of Gelsolin and Cofilin1, it appears that continuous upregulation of actin severing activity in hypertrophic adipocytes might be responsible for the downregulation of F/G-actin ratio and subsequent attenuation of insulin-dependent glucose uptake ability. Conversely, it is possible that downregulation of actin severing enzymes in brown/beige adipocytes might result in intrinsic features of well organized F-actin and potentiated insulin-dependent glucose uptake ability than white adipocytes. Thus, these data suggest that different insulin-stimulated glucose uptake ability between white and brown/beige adipocytes would be derived from distinct F/G-actin dynamics-mediated GLUT4 trafficking upon insulin. Nonetheless, further studies are needed to identify the upstream transcriptional or post-translational regulators for actin-severing genes in adipocytes.

Here, I propose a novel role of adipocyte morphology with different LD configuration in the regulation of insulin-dependent glucose uptake. In adipocytes, LD size and locularity are variable and reversible upon

physiological and pathological conditions. Differences in LD configuration could affect cytosolic space and modulate F/G-actin dynamics, leading to control insulin-stimulated GSVs trafficking and glucose uptake in adipocytes. Consequently, in adipocytes, LD multilocularization improves insulin-dependent glucose uptake while LD unilocularization provokes insulin-dependent glucose uptake (Fig. 28). Collectively, these data revealed the physiological significance that dynamic LD transformation in adipocytes would be a novel mechanism of adipocyte to determine its energy handling capacity by modulating F/G-actin dynamics.

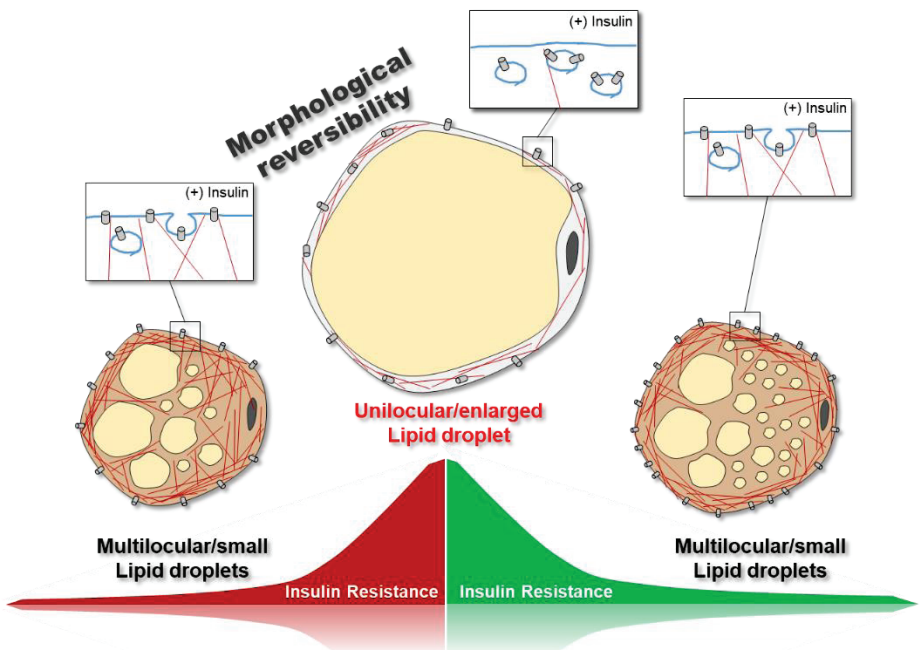

Figure 28. Graphical summary illustrating LD morphology-dependent insulin sensitivity control. Relationship among LD morphology, F/G-actin dynamics, and GSVs trafficking in adipocytes.

CONCLUSION AND PERSPECTIVES

Insulin resistance is a major risk factor for the etiology of metabolic diseases such as type 2 diabetes, hyperlipidemia, hypertension, and cardiovascular diseases. Since obesity-induced increase of adiposity and insulin resistance are tightly associated, numerous studies have been conducted to understand the relationship between the two phenomena. Of numerous causes of insulin resistance, adipocyte hypertrophy and inflammatory responses in adipose tissue remodeling have been recently considered as key factors for insulin resistance. In particular, adipocyte hypertrophy has long been known to be closely associated with metabolically negative phenomena. However, it is not yet clear how adipocyte hypertrophy could cause insulin resistance in obesity. Due to the interactions between various cells constituting adipose tissues (ATs), it has been technically difficult to study underlying mechanisms of adipocyte hypertrophy-induced insulin resistance. Furthermore, the question of why enlarged adipocytes are metabolically bad has been remained elusive. In the first chapter, I demonstrated that unilocularization of LD and enlargement of LD in adipocyte hypertrophy *per se* could deteriorate insulin resistance through repression of insulin-stimulated GLUT4 trafficking in an inflammation independent manner. In the second chapter, I further investigated the roles of adipocyte LDs in the regulation of insulin sensitivity and found that reversible changes of LD locularity could affect insulin-dependent GLUT4 translocation

to plasma membrane through modulation of F/G-actin dynamics. Together, these results provide novel aspects of the roles of LD locularity and size in adipocytes in the regulation of insulin sensitivity under physiological and pathological conditions.

1. Adipocyte hypertrophy *per se* provoke insulin resistance

Despite of numerous studies, the answer to the simple question of why big adipocytes are bad in terms of insulin sensitivity has not been properly addressed. In obesity, ATs dynamically increase the size and/or number of adipocytes. In addition, AT stromal vascular cells (SVCs), such as macrophages, T-cells, and B-cells, dramatically change toward pro-inflammatory state in obesity. These series of events are called “adipose tissue remodeling”, and have been considered to confer insulin resistance[6]. In this study, adipocyte hypertrophy accompanied with LD unilocularization and enlargement *per se* could aggravate insulin resistance without any changes of insulin signaling cascades (Fig. 3, 6A, and 8). These results suggest that there might be a mechanism to regulate insulin sensitivity by intrinsic changes in the LD morphology independent of insulin downstream signaling pathway.

2. In early obesity, inflammation is dissociated from insulin resistance

In obese ATs, chronic and low-grade inflammation have been implicated in insulin resistance[20,21]. Recent studies have shown that insulin resistance also appears in the early stages of obesity, and in this case, pro-inflammatory changes in AT are not essential for insulin resistance[26-30]. In accordance with the previous reports, I observed insulin resistance without pro-inflammatory response *in vitro* and *in vivo* unilocular enlarged adipocytes. Collectively, these emerging evidences suggest that AT inflammation, which is one of the major factors of insulin resistance in severe obesity, might be dissociated from adipocyte hypertrophy-induced insulin resistance in the early stages of obesity. These data also indicate that adipocyte hypertrophy might play crucial roles in priming of obesity-induced insulin resistance in a cell autonomous manner.

3. Intrinsic reversibility of LD locularity and size affect adipocyte insulin sensitivity

Current data suggest that insulin sensitivity of adipocytes is closely related to the number and size of LDs in adipocytes (Fig. 9 and 10C). Recently, it has been reported that active BAT is present in humans and that BAT absorbs

large amounts of glucose compared to WAT[76,77]. Morphologies of adipocytes in different ATs are considerably distinct depending on their anatomical locations. Most white adipocytes are unilocular while brown/beige adipocytes are multilocular. In this regard, it is plausible to speculate that LD morphological differences might be attributable to functional variations between white and brown adipocytes. Here, I observed that adipocytes with small and multilocular LDs exhibited better insulin-dependent glucose uptake ability, whereas adipocytes with unilocular and enlarged LD showed less ability of glucose uptake upon insulin. Together, I would like to propose that adipocytes LD locularity and size, and insulin-dependent glucose uptake ability are dramatically and modulated by physiological conditions such as cold-exposure or thermoneutrality.

4. F/G-actin dynamics mediate insulin sensitivity control upon LD locularity changes

In accordance with morphological and actin cytoskeletal differences, multilocular adipocytes showed higher insulin-dependent glucose uptake capacity with increased GLUT4 translocation than unilocular adipocytes, implying that LD locularity and glucose uptake ability might be closely linked each other through F/G-actin dynamics. Also, I observed that administration of actin polymerization inhibitor, cytochalasin D, to mice resulted in

downregulation of adipose tissue F/G-actin dynamics and provoked systemic insulin resistance. In pharmacological actin disruption-induced insulin resistance, insufficient insulin-stimulated glucose absorption in ATs would contribute to systemic insulin resistance. These results indicate important roles of actin cytoskeletal dynamics in mediating effects of morphological changes of adipocytes on insulin sensitivity control. Taken together, these results suggest that the close relationship between F/G-actin dynamics and LD morphology would act as one of key factors determining adipocyte-autonomous control of insulin sensitivity.

REFERENCE

1 Wang, G. Raison d'etre of insulin resistance: the adjustable threshold hypothesis. *J R Soc Interface* **11**, 20140892, doi:10.1098/rsif.2014.0892 (2014).

2 Kahn, B. B. & Flier, J. S. Obesity and insulin resistance. *J Clin Invest* **106**, 473-481, doi:10.1172/JCI10842 (2000).

3 Haslam, D. W. & James, W. P. Obesity. *Lancet* **366**, 1197-1209, doi:10.1016/S0140-6736(05)67483-1 (2005).

4 Luppino, F. S. *et al.* Overweight, obesity, and depression: a systematic review and meta-analysis of longitudinal studies. *Arch Gen Psychiatry* **67**, 220-229, doi:10.1001/archgenpsychiatry.2010.2 (2010).

5 Birsoy, K., Festuccia, W. T. & Laplante, M. A comparative perspective on lipid storage in animals. *J Cell Sci* **126**, 1541-1552, doi:10.1242/jcs.104992 (2013).

6 Huh, J. Y., Park, Y. J., Ham, M. & Kim, J. B. Crosstalk between adipocytes and immune cells in adipose tissue inflammation and metabolic dysregulation in obesity. *Mol Cells* **37**, 365-371, doi:10.14348/molcells.2014.0074 (2014).

7 Birbrair, A. *et al.* Role of pericytes in skeletal muscle regeneration and fat accumulation. *Stem Cells Dev* **22**, 2298-2314, doi:10.1089/scd.2012.0647 (2013).

8 Klaus, S., Ely, M., Encke, D. & Heldmaier, G. Functional assessment of white and brown adipocyte development and energy metabolism in cell culture. Dissociation of terminal differentiation and thermogenesis in brown adipocytes. *J Cell Sci* **108 (Pt 10)**, 3171-3180 (1995).

9 Klaus, S., Casteilla, L., Bouillaud, F. & Ricquier, D. The uncoupling protein UCP: a membraneous mitochondrial ion carrier exclusively expressed in brown adipose tissue. *Int J Biochem* **23**, 791-801 (1991).

10 Ricquier, D., Casteilla, L. & Bouillaud, F. Molecular studies of the uncoupling protein. *FASEB J* **5**, 2237-2242 (1991).

11 Rondinone, C. M. *et al.* Insulin receptor substrate (IRS) 1 is reduced and IRS-2 is the main docking protein for phosphatidylinositol 3-kinase in adipocytes from subjects with non-insulin-dependent diabetes mellitus. *Proc Natl Acad Sci U S A* **94**, 4171-4175 (1997).

12 Shepherd, P. R. & Kahn, B. B. Glucose transporters and insulin action--implications for insulin resistance and diabetes mellitus. *N Engl J Med* **341**, 248-257, doi:10.1056/NEJM199907223410406 (1999).

13 Stockli, J., Fazakerley, D. J. & James, D. E. GLUT4 exocytosis. *J Cell Sci* **124**, 4147-4159, doi:10.1242/jcs.097063 (2011).

14 Kershaw, E. E. & Flier, J. S. Adipose tissue as an endocrine organ. *J Clin Endocrinol Metab* **89**, 2548-2556, doi:10.1210/jc.2004-0395 (2004).

15 Wang, Q. A., Tao, C., Gupta, R. K. & Scherer, P. E. Tracking adipogenesis during white adipose tissue development, expansion and regeneration. *Nature medicine* **19**, 1338-1344, doi:10.1038/nm.3324 (2013).

16 Martinsson, A. Hypertrophy and hyperplasia of human adipose tissue in obesity. *Polskie Archiwum Medycyny Wewnetrznej* **42**, 481-486 (1969).

17 Weisberg, S. P. *et al.* Obesity is associated with macrophage accumulation in adipose tissue. *J Clin Invest* **112**, 1796-1808, doi:10.1172/JCI19246 (2003).

18 Xu, H. *et al.* Chronic inflammation in fat plays a crucial role in the development of obesity-related insulin resistance. *J Clin Invest* **112**, 1821-1830, doi:10.1172/JCI19451 (2003).

19 Ceddia, R. B., Koistinen, H. A., Zierath, J. R. & Sweeney, G. Analysis of paradoxical observations on the association between leptin and insulin resistance. *FASEB J* **16**, 1163-1176, doi:10.1096/fj.02-0158rev (2002).

20 Lumeng, C. N., Bodzin, J. L. & Saltiel, A. R. Obesity induces a phenotypic switch in adipose tissue macrophage polarization. *J Clin Invest* **117**, 175-184, doi:10.1172/JCI29881 (2007).

21 Odegaard, J. I. & Chawla, A. Mechanisms of macrophage activation in obesity-induced insulin resistance. *Nature clinical practice. Endocrinology & metabolism* **4**, 619-626, doi:10.1038/ncpendmet0976 (2008).

22 Hirosumi, J. *et al.* A central role for JNK in obesity and insulin resistance. *Nature* **420**, 333-336, doi:10.1038/nature01137 (2002).

23 Yuan, M. *et al.* Reversal of obesity- and diet-induced insulin resistance with salicylates or targeted disruption of Ikkbeta. *Science* **293**, 1673-1677, doi:10.1126/science.1061620 (2001).

24 Kim, J. K. *et al.* Prevention of fat-induced insulin resistance by salicylate. *J Clin Invest* **108**, 437-446, doi:10.1172/JCI11559 (2001).

25 Arkan, M. C. *et al.* IKK-beta links inflammation to obesity-induced insulin resistance. *Nature medicine* **11**, 191-198, doi:10.1038/nm1185 (2005).

26 Sears, D. D. *et al.* 12/15-lipoxygenase is required for the early onset of high fat diet-induced adipose tissue inflammation and insulin resistance in mice. *PloS one* **4**, e7250, doi:10.1371/journal.pone.0007250 (2009).

27 Kleemann, R. *et al.* Time-resolved and tissue-specific systems analysis of the pathogenesis of insulin resistance. *PloS one* **5**, e8817, doi:10.1371/journal.pone.0008817 (2010).

28 Lee, Y. S. *et al.* Inflammation is necessary for long-term but not short-term high-fat diet-induced insulin resistance. *Diabetes* **60**, 2474-2483, doi:10.2337/db11-0194 (2011).

29 Wiedemann, M. S. *et al.* Short-term HFD does not alter lipolytic function of adipocytes. *Adipocyte* **3**, 115-120, doi:10.4161/adip.27575 (2014).

30 Wiedemann, M. S., Wueest, S., Item, F., Schoenle, E. J. & Konrad, D. Adipose tissue inflammation contributes to short-term high-fat diet-

induced hepatic insulin resistance. *American journal of physiology. Endocrinology and metabolism* **305**, E388-395, doi:10.1152/ajpendo.00179.2013 (2013).

31 Sciacqua, A., Marini, M. A., Hribal, M. L., Perticone, F. & Sesti, G. Association of insulin resistance indexes to carotid intima-media thickness. *PloS one* **8**, e53968, doi:10.1371/journal.pone.0053968 (2013).

32 Dalmas, E. *et al.* Intima-media thickness in severe obesity: links with BMI and metabolic status but not with systemic or adipose tissue inflammation. *Diabetes care* **36**, 3793-3802, doi:10.2337/dc13-0256 (2013).

33 Gao, H. *et al.* Early B cell factor 1 regulates adipocyte morphology and lipolysis in white adipose tissue. *Cell metabolism* **19**, 981-992, doi:10.1016/j.cmet.2014.03.032 (2014).

34 Shoelson, S. E., Herrero, L. & Naaz, A. Obesity, inflammation, and insulin resistance. *Gastroenterology* **132**, 2169-2180, doi:10.1053/j.gastro.2007.03.059 (2007).

35 Kubota, N. *et al.* PPAR gamma mediates high-fat diet-induced adipocyte hypertrophy and insulin resistance. *Molecular cell* **4**, 597-609 (1999).

36 Park, J., Lee, H. Y., Cho, M. H. & Park, S. B. Development of a cy3-labeled glucose bioprobe and its application in bioimaging and screening for anticancer agents. *Angewandte Chemie* **46**, 2018-2022, doi:10.1002/anie.200604364 (2007).

37 Brenner, R. R., Vazza, D. V. & Detomas, M. E. Effect of a Fat-Free Diet and of Different Dietary Fatty Acids (Palmitate, Oleate, and Linoleate) on the Fatty Acid Composition of Fresh-Water Fish Lipids. *Journal of lipid research* **4**, 341-345 (1963).

38 Psychogios, N. *et al.* The human serum metabolome. *PloS one* **6**, e16957, doi:10.1371/journal.pone.0016957 (2011).

39 Nguyen, M. T. *et al.* JNK and tumor necrosis factor-alpha mediate free fatty acid-induced insulin resistance in 3T3-L1 adipocytes. *The*

Journal of biological chemistry **280**, 35361-35371, doi:10.1074/jbc.M504611200 (2005).

40 Staiger, H. *et al.* Palmitate-induced interleukin-6 expression in human coronary artery endothelial cells. *Diabetes* **53**, 3209-3216 (2004).

41 Schiller, Z. A., Schiele, N. R., Sims, J. K., Lee, K. & Kuo, C. K. Adipogenesis of adipose-derived stem cells may be regulated via the cytoskeleton at physiological oxygen levels in vitro. *Stem cell research & therapy* **4**, 79, doi:10.1186/scrt230 (2013).

42 Feng, T., Szabo, E., Dziak, E. & Opas, M. Cytoskeletal disassembly and cell rounding promotes adipogenesis from ES cells. *Stem cell reviews* **6**, 74-85, doi:10.1007/s12015-010-9115-8 (2010).

43 Hong, C. & Tontonoz, P. Coordination of inflammation and metabolism by PPAR and LXR nuclear receptors. *Current opinion in genetics & development* **18**, 461-467, doi:10.1016/j.gde.2008.07.016 (2008).

44 Koh, Y. J. *et al.* Activation of PPAR gamma induces profound multilocularization of adipocytes in adult mouse white adipose tissues. *Experimental & molecular medicine* **41**, 880-895, doi:10.3858/emm.2009.41.12.094 (2009).

45 Wernstedt Asterholm, I. *et al.* Adipocyte inflammation is essential for healthy adipose tissue expansion and remodeling. *Cell metabolism* **20**, 103-118, doi:10.1016/j.cmet.2014.05.005 (2014).

46 Jernas, M. *et al.* Separation of human adipocytes by size: hypertrophic fat cells display distinct gene expression. *FASEB J* **20**, 1540-1542, doi:10.1096/fj.05-5678fje (2006).

47 Bluher, M. *et al.* Role of insulin action and cell size on protein expression patterns in adipocytes. *The Journal of biological chemistry* **279**, 31902-31909, doi:10.1074/jbc.M404570200 (2004).

48 Haller, H., Leonhardt, W., Hanefeld, M. & Julius, U. Relationship between adipocyte hypertrophy and metabolic disturbances. *Endokrinologie* **74**, 63-72 (1979).

49 Davidson, M. B. Insulin sensitivity of the large human adipocyte in vitro. *Diabetes* **24**, 1086-1093 (1975).

50 Hoehn, K. L. *et al.* IRS1-independent defects define major nodes of insulin resistance. *Cell metabolism* **7**, 421-433, doi:10.1016/j.cmet.2008.04.005 (2008).

51 Yeop Han, C. *et al.* Differential effect of saturated and unsaturated free fatty acids on the generation of monocyte adhesion and chemotactic factors by adipocytes: dissociation of adipocyte hypertrophy from inflammation. *Diabetes* **59**, 386-396, doi:10.2337/db09-0925 (2010).

52 Han, C. Y. *et al.* Adipocyte-derived serum amyloid A3 and hyaluronan play a role in monocyte recruitment and adhesion. *Diabetes* **56**, 2260-2273, doi:10.2337/db07-0218 (2007).

53 Suganami, T. *et al.* Role of the Toll-like receptor 4/NF-kappaB pathway in saturated fatty acid-induced inflammatory changes in the interaction between adipocytes and macrophages. *Arteriosclerosis, thrombosis, and vascular biology* **27**, 84-91, doi:10.1161/01.ATV.0000251608.09329.9a (2007).

54 Ajuwon, K. M. & Spurlock, M. E. Palmitate activates the NF-kappaB transcription factor and induces IL-6 and TNFalpha expression in 3T3-L1 adipocytes. *The Journal of nutrition* **135**, 1841-1846 (2005).

55 Bradley, R. L., Fisher, F. F. & Maratos-Flier, E. Dietary fatty acids differentially regulate production of TNF-alpha and IL-10 by murine 3T3-L1 adipocytes. *Obesity* **16**, 938-944, doi:10.1038/oby.2008.39 (2008).

56 Brozinick, J. T., Jr., Hawkins, E. D., Strawbridge, A. B. & Elmendorf, J. S. Disruption of cortical actin in skeletal muscle demonstrates an essential role of the cytoskeleton in glucose transporter 4 translocation in insulin-sensitive tissues. *The Journal of biological chemistry* **279**, 40699-40706, doi:10.1074/jbc.M402697200 (2004).

57 Rivero, F. *et al.* The role of the cortical cytoskeleton: F-actin crosslinking proteins protect against osmotic stress, ensure cell size,

cell shape and motility, and contribute to phagocytosis and development. *J Cell Sci* **109 (Pt 11)**, 2679-2691 (1996).

58 James, D. E., Strube, M. & Mueckler, M. Molecular cloning and characterization of an insulin-regulatable glucose transporter. *Nature* **338**, 83-87, doi:10.1038/338083a0 (1989).

59 Birnbaum, M. J. Identification of a novel gene encoding an insulin-responsive glucose transporter protein. *Cell* **57**, 305-315 (1989).

60 James, D. E., Brown, R., Navarro, J. & Pilch, P. F. Insulin-regulatable tissues express a unique insulin-sensitive glucose transport protein. *Nature* **333**, 183-185, doi:10.1038/333183a0 (1988).

61 Abel, E. D. *et al.* Adipose-selective targeting of the GLUT4 gene impairs insulin action in muscle and liver. *Nature* **409**, 729-733, doi:10.1038/35055575 (2001).

62 Shepherd, P. R. *et al.* Adipose cell hyperplasia and enhanced glucose disposal in transgenic mice overexpressing GLUT4 selectively in adipose tissue. *The Journal of biological chemistry* **268**, 22243-22246 (1993).

63 Akira, S. & Takeda, K. Toll-like receptor signalling. *Nature reviews. Immunology* **4**, 499-511, doi:10.1038/nri1391 (2004).

64 Poltorak, A. *et al.* Defective LPS signaling in C3H/HeJ and C57BL/10ScCr mice: mutations in Tlr4 gene. *Science* **282**, 2085-2088 (1998).

65 Shi, H. *et al.* TLR4 links innate immunity and fatty acid-induced insulin resistance. *J Clin Invest* **116**, 3015-3025, doi:10.1172/JCI28898 (2006).

66 Tsukumo, D. M. *et al.* Loss-of-function mutation in Toll-like receptor 4 prevents diet-induced obesity and insulin resistance. *Diabetes* **56**, 1986-1998, doi:10.2337/db06-1595 (2007).

67 Suganami, T. *et al.* Attenuation of obesity-induced adipose tissue inflammation in C3H/HeJ mice carrying a Toll-like receptor 4 mutation. *Biochemical and biophysical research communications* **354**, 45-49, doi:10.1016/j.bbrc.2006.12.190 (2007).

68 Poggi, M. *et al.* C3H/HeJ mice carrying a toll-like receptor 4 mutation are protected against the development of insulin resistance in white adipose tissue in response to a high-fat diet. *Diabetologia* **50**, 1267-1276, doi:10.1007/s00125-007-0654-8 (2007).

69 Vijay-Kumar, M. *et al.* Loss of function mutation in toll-like receptor-4 does not offer protection against obesity and insulin resistance induced by a diet high in trans fat in mice. *Journal of inflammation* **8**, 2, doi:10.1186/1476-9255-8-2 (2011).

70 Choe, S. S. *et al.* Macrophage HIF-2alpha ameliorates adipose tissue inflammation and insulin resistance in obesity. *Diabetes* **63**, 3359-3371, doi:10.2337/db13-1965 (2014).

71 Harms, M. & Seale, P. Brown and beige fat: development, function and therapeutic potential. *Nature medicine* **19**, 1252-1263, doi:10.1038/nm.3361 (2013).

72 Wu, J., Cohen, P. & Spiegelman, B. M. Adaptive thermogenesis in adipocytes: is beige the new brown? *Genes Dev* **27**, 234-250, doi:10.1101/gad.211649.112 (2013).

73 Wu, J. *et al.* Beige adipocytes are a distinct type of thermogenic fat cell in mouse and human. *Cell* **150**, 366-376, doi:10.1016/j.cell.2012.05.016 (2012).

74 Aldiss, P. *et al.* Exercise-induced 'browning' of adipose tissues. *Metabolism* **81**, 63-70, doi:10.1016/j.metabol.2017.11.009 (2018).

75 Enerback, S. The origins of brown adipose tissue. *N Engl J Med* **360**, 2021-2023, doi:10.1056/NEJMcibr0809610 (2009).

76 van Marken Lichtenbelt, W. D. *et al.* Cold-activated brown adipose tissue in healthy men. *N Engl J Med* **360**, 1500-1508, doi:10.1056/NEJMoa0808718 (2009).

77 Cypess, A. M. *et al.* Identification and importance of brown adipose tissue in adult humans. *N Engl J Med* **360**, 1509-1517, doi:10.1056/NEJMoa0810780 (2009).

78 Daikoku, T., Shinohara, Y., Shima, A., Yamazaki, N. & Terada, H. Specific elevation of transcript levels of particular protein subtypes

induced in brown adipose tissue by cold exposure. *Biochim Biophys Acta* **1457**, 263-272 (2000).

79 Heine, M. *et al.* Lipolysis Triggers a Systemic Insulin Response Essential for Efficient Energy Replenishment of Activated Brown Adipose Tissue in Mice. *Cell metabolism* **28**, 644-655 e644, doi:10.1016/j.cmet.2018.06.020 (2018).

80 Wang, X. & Wahl, R. Responses of the insulin signaling pathways in the brown adipose tissue of rats following cold exposure. *PloS one* **9**, e99772, doi:10.1371/journal.pone.0099772 (2014).

81 Roberts-Toler, C., O'Neill, B. T. & Cypess, A. M. Diet-induced obesity causes insulin resistance in mouse brown adipose tissue. *Obesity* **23**, 1765-1770, doi:10.1002/oby.21134 (2015).

82 Cui, X. *et al.* Thermoneutrality decreases thermogenic program and promotes adiposity in high-fat diet-fed mice. *Physiol Rep* **4**, doi:10.14814/phy2.12799 (2016).

83 Vitali, A. *et al.* The adipose organ of obesity-prone C57BL/6J mice is composed of mixed white and brown adipocytes. *Journal of lipid research* **53**, 619-629, doi:10.1194/jlr.M018846 (2012).

84 Bartelt, A. & Heeren, J. Adipose tissue browning and metabolic health. *Nat Rev Endocrinol* **10**, 24-36, doi:10.1038/nrendo.2013.204 (2014).

85 Wallberg-Henriksson, H. & Zierath, J. R. Metabolism. Exercise remodels subcutaneous fat tissue and improves metabolism. *Nat Rev Endocrinol* **11**, 198-200, doi:10.1038/nrendo.2015.24 (2015).

86 Cohen, P. *et al.* Ablation of PRDM16 and beige adipose causes metabolic dysfunction and a subcutaneous to visceral fat switch. *Cell* **156**, 304-316, doi:10.1016/j.cell.2013.12.021 (2014).

87 Kanzaki, M., Furukawa, M., Raab, W. & Pessin, J. E. Phosphatidylinositol 4,5-bisphosphate regulates adipocyte actin dynamics and GLUT4 vesicle recycling. *The Journal of biological chemistry* **279**, 30622-30633, doi:10.1074/jbc.M401443200 (2004).

88 Kanzaki, M., Watson, R. T., Khan, A. H. & Pessin, J. E. Insulin stimulates actin comet tails on intracellular GLUT4-containing compartments in

differentiated 3T3L1 adipocytes. *The Journal of biological chemistry* **276**, 49331-49336, doi:10.1074/jbc.M109657200 (2001).

89 Kao, A. W., Noda, Y., Johnson, J. H., Pessin, J. E. & Saltiel, A. R. Aldolase mediates the association of F-actin with the insulin-responsive glucose transporter GLUT4. *The Journal of biological chemistry* **274**, 17742-17747 (1999).

90 Leto, D. & Saltiel, A. R. Regulation of glucose transport by insulin: traffic control of GLUT4. *Nat Rev Mol Cell Biol* **13**, 383-396, doi:10.1038/nrm3351 (2012).

91 Ng, Y., Ramm, G., Lopez, J. A. & James, D. E. Rapid activation of Akt2 is sufficient to stimulate GLUT4 translocation in 3T3-L1 adipocytes. *Cell metabolism* **7**, 348-356, doi:10.1016/j.cmet.2008.02.008 (2008).

92 Miinea, C. P. *et al.* AS160, the Akt substrate regulating GLUT4 translocation, has a functional Rab GTPase-activating protein domain. *Biochem J* **391**, 87-93, doi:10.1042/BJ20050887 (2005).

93 Calera, M. R. *et al.* Insulin increases the association of Akt-2 with Glut4-containing vesicles. *The Journal of biological chemistry* **273**, 7201-7204 (1998).

94 Sano, H. *et al.* Insulin-stimulated phosphorylation of a Rab GTPase-activating protein regulates GLUT4 translocation. *The Journal of biological chemistry* **278**, 14599-14602, doi:10.1074/jbc.C300063200 (2003).

95 Stenbit, A. E. *et al.* Diverse effects of Glut 4 ablation on glucose uptake and glycogen synthesis in red and white skeletal muscle. *J Clin Invest* **98**, 629-634, doi:10.1172/JCI118833 (1996).

96 Brozinick, J. T., Jr. *et al.* GLUT4 overexpression in db/db mice dose-dependently ameliorates diabetes but is not a lifelong cure. *Diabetes* **50**, 593-600 (2001).

97 Treadway, J. L. *et al.* Enhanced peripheral glucose utilization in transgenic mice expressing the human GLUT4 gene. *The Journal of biological chemistry* **269**, 29956-29961 (1994).

98 Gunning, P. W., Ghoshdastider, U., Whitaker, S., Popp, D. & Robinson, R. C. The evolution of compositionally and functionally distinct actin filaments. *J Cell Sci* **128**, 2009-2019, doi:10.1242/jcs.165563 (2015).

99 Schmidt, A. & Hall, M. N. Signaling to the actin cytoskeleton. *Annu Rev Cell Dev Biol* **14**, 305-338, doi:10.1146/annurev.cellbio.14.1.305 (1998).

100 Spiegelman, B. M. & Farmer, S. R. Decreases in tubulin and actin gene expression prior to morphological differentiation of 3T3 adipocytes. *Cell* **29**, 53-60 (1982).

101 Yang, W. *et al.* Arp2/3 complex regulates adipogenesis by controlling cortical actin remodelling. *Biochem J* **464**, 179-192, doi:10.1042/BJ20140805 (2014).

102 Spiegelman, B. M. & Ginty, C. A. Fibronectin modulation of cell shape and lipogenic gene expression in 3T3-adipocytes. *Cell* **35**, 657-666 (1983).

103 Park, J. *et al.* Increase in glucose-6-phosphate dehydrogenase in adipocytes stimulates oxidative stress and inflammatory signals. *Diabetes* **55**, 2939-2949, doi:10.2337/db05-1570 (2006).

104 Mahajan, R. D. & Patra, S. K. Irisin, a novel myokine responsible for exercise induced browning of white adipose tissue. *Indian J Clin Biochem* **28**, 102-103, doi:10.1007/s12291-012-0255-2 (2013).

105 Ashwell, M., Jennings, G., Richard, D., Stirling, D. M. & Trayhurn, P. Effect of acclimation temperature on the concentration of the mitochondrial 'uncoupling' protein measured by radioimmunoassay in mouse brown adipose tissue. *FEBS Lett* **161**, 108-112 (1983).

106 Lee, H. Y., Lee, J. J., Park, J. & Park, S. B. Development of fluorescent glucose bioprobes and their application on real-time and quantitative monitoring of glucose uptake in living cells. *Chemistry* **17**, 143-150, doi:10.1002/chem.201002560 (2011).

107 Kim, J. I. *et al.* Lipid-overloaded enlarged adipocytes provoke insulin resistance independent of inflammation. *Mol Cell Biol* **35**, 1686-1699, doi:10.1128/MCB.01321-14 (2015).

108 Southwick, F. S. Gelsolin and ADF/cofilin enhance the actin dynamics of motile cells. *Proc Natl Acad Sci U S A* **97**, 6936-6938 (2000).

109 van Rheenen, J., Condeelis, J. & Glogauer, M. A common cofilin activity cycle in invasive tumor cells and inflammatory cells. *J Cell Sci* **122**, 305-311, doi:10.1242/jcs.031146 (2009).

110 Ressad, F. *et al.* Kinetic analysis of the interaction of actin-depolymerizing factor (ADF)/cofilin with G- and F-actins. Comparison of plant and human ADFs and effect of phosphorylation. *The Journal of biological chemistry* **273**, 20894-20902 (1998).

111 Azeez, O. I., Meintjes, R. & Chamunorwa, J. P. Fat body, fat pad and adipose tissues in invertebrates and vertebrates: the nexus. *Lipids Health Dis* **13**, 71, doi:10.1186/1476-511X-13-71 (2014).

112 Nikami, H., Shimizu, Y., Endoh, D., Yano, H. & Saito, M. Cold exposure increases glucose utilization and glucose transporter expression in brown adipose tissue. *Biochemical and biophysical research communications* **185**, 1078-1082 (1992).

113 Shimizu, Y. *et al.* Increased expression of glucose transporter GLUT-4 in brown adipose tissue of fasted rats after cold exposure. *Am J Physiol* **264**, E890-895, doi:10.1152/ajpendo.1993.264.6.E890 (1993).

114 Patki, V. *et al.* Insulin action on GLUT4 traffic visualized in single 3T3-l1 adipocytes by using ultra-fast microscopy. *Mol Biol Cell* **12**, 129-141, doi:10.1091/mbc.12.1.129 (2001).

국문 초록

지방조직은 체내 에너지 항상성을 조절하는 주요 장기 중 하나이다. 지방조직은 해부학적 위치와 기능을 기준으로 크게 백색내장지방, 백색피하지방, 그리고 갈색지방으로 구분할 수 있다. 지방조직의 주요 기능 중 하나는 인슐린에 반응하여 체내 잉여 에너지를 흡수하여 중성지방대사물을 지방소체에 저장하는 것이다. 인슐린 자극에 대한 세포의 적절한 반응성을 인슐린 민감도라 한다. 반대로 인슐린 자극이 존재함에도 불구하고 세포가 이에 적절하게 반응하지 못하는 경우를 인슐린 저항성이라 정의한다. 인슐린 저항성은 다양한 대사 질환의 주요 발병 원인으로 인식된다. 다양한 생리적 혹은 병리적 상황에서 지방세포는 인슐린에 대한 반응성과 형태학적 변화를 수반한다. 지방조직은 지방세포와 면역세포들을 포함하는 맥관계 간세포들(stromal vascular cells)로 이루어져 있으며, 이들 사이에는 복잡한 세포간 상호작용이 존재한다. 이러한 이유로 대사질환, 특히, 인슐린저항성 유발 측면에서 지방조직이 중요함에도 불구하고, 지방세포 내재적 원인에 의한 인슐린 민감도 조절기전에 대해서는 연구가 부족한 상황이다. 따라서, 본 학위논문 연구에서는 지방세포의 형태와 인슐린 반응성의 상호관계에 초점을 맞추고 지방세포 형태적 변화가 기능적 변화를 수반하는 기전에 대해 연구하였다.

본 논문의 1 장에서는 비만이 유도된 개체에서 단일지방소체 크기 증가에 의한 지방세포 거대화 현상과 인슐린 저항성이 유발되는 기전에 대해 조사하기 위해, 다양한 자유지방산을 분화된 3T3-L1 지방세포에 처리함으로써 거대 지방세포 모델을 구축하였다. 올레산 (Oleic acid)을 처리하여 유도한 거대지방세포의 경우, 염증반응 및 인슐린 하위 신호전달과정과 독립적으로 인슐린 저항성이 발생하였다. 또한, 현미경기법을 활용한 단일세포수준에서의 관찰을 통해, 거대 지방세포 특이적으로 인슐린의존적 포도당 수송체 4 의 이동이 저해되었으며, 이 때 세포막에 인접한 액틴섬유구조가 손상되어 있음을 관찰하였다.

본 논문의 2 장에서는 지방소체 수적 변화에 의한 인슐린 의존적 포도당 흡수능에 대한 기전을 조사하기 위해 올레산 처리를 통해 1) 중성지방 축적에 의한 지방소체 단일화와 거대화를 유도한 경우 그리고 2) 거대화 유도 후 축적된 중성지방의 분해를 통해 지방소체 수를 다시 늘려준 경우, 각각에서 인슐린의존적 포도당 흡수능 및 포도당 수송체 4 의 이동능력을 측정하였다. 지방소체의 수적 증가와 크기 감소가 유도되는 생리적 조건들 (추위자극/베타아드레날린 자극)에서는 인슐린 의존적 포도당 흡수 및 포도당 수송체 4 의 이동이 증가한 반면 지방소체 단일화 혹은 거대화가 유도되는 생리적 (thermoneutral condition) 또는 병리적 (비만) 조건에서는 인슐린 의존적 포도당 흡수 및 포도당 수송체 4 의 이동이 저해되었다. 각 조건에서 지방세포 내 F 액틴과

G 액틴간의 비율이 역동적으로 변화됨을 관찰하였고 이를 통해 F/G 액틴 비율 변화에 의한 인슐린 의존적 포도당 수송체 4 이동 조절이 형태적 변화에 따른 지방세포 인슐린 의존적 포도당 흡수 과정을 매개하는 주요 기전 중 하나임을 새로이 제시하였다.

본 연구를 통하여 1) 지방소체의 크기 및 수적 변화를 동반하는 형태 변화가 지방세포 피질 부위의 액틴 세포골격 구조를 조절함과 2) F 액틴/G 액틴간의 역동적 변화가 인슐린 의존적 포도당 수송체 4 이동을 조절함을 규명하였고, 이를 통해 지방세포 형태 변화가 지방세포 인슐린 민감도를 직접 조절하는 기전임을 새로이 제안하였다. 특히, 이러한 조절 기전은 세포수준에서의 세포 본연의 형태 변화가 조직 및 개체의 대사과정에 영향을 미칠 수 있음을 제시하였다는 점에서 큰 의미를 지니며, 비만 혹은 운동 등 다양한 생리적 병리적 조건에 따른 지방세포 기능 조절에 있어 지방세포의 형태 조절이 중요한 역할을 할 수 있음을 암시한다.

주요어: 지방세포, 지방조직, 비만, 인슐린, 인슐린 저항성, 인슐린 민감도, 액틴세포골격, 포도당, 포도당수송체 4

학번: 2009-20326

감사의 글

저의 학위기간을 묵묵히 응원해 주셨던 모든 분들께 이 글을 바칩니다. 스무살 새내기에서 이십대 중반을 지나 이제 삼십대 중반에 접어들고 있는 저는 드디어 과학자로서 한 단계 성장하였음을 증명하는 박사학위를 받게 되었습니다. 꿈에 그리던 대학 원하던 과에 합격하여 과학자의 길을 걸으며 지금까지 공부를 계속할 수 있었던 것은 모두 저의 가족들 그리고 가족 못지 않게 소중한 주위 동료들 덕분이었습니다. 이 지면을 통해 저의 소중한 여러분들께 감사로 가득한 제 마음이 전해지기를 바랍니다. 뿐만 아니라 학위과정 동안 전폭적으로 지원해 주시고 지도해 주신 김재범 교수님 그리고 저의 박사학위심사를 맡아주셨던 이건수 교수님, 구승회 교수님, 박승범 교수님, 김진홍 교수님께도 감사의 말씀 전합니다.

지난 10 년의 학위기간 동안 참 많은 일들이 있었습니다. 연구에 관련하여 어려움에 봉착한 적도 많았고 제 소중한 가족에게 어려움이 발생한 적도 있었습니다. 그럴때 마다 바로 곁에서 제가 꿈을 지킬 수 있도록 기다려주시고 버텨주시고 이겨내주셨던 저의 부모님과 제 동생 효진이에게 진심으로 고맙고 사랑한다는 말 전하고 싶습니다. 그리고 저의 어려운 상황들을 지혜롭게 이겨낼 수 있도록 옆에서 묵묵히 도와주셨던 김재범 선생님께도 항상 말로 담기 힘들 만큼 감사할 따름입니다.

수학하는 기간 함께 웃고 울어 주었던 연구실 동료들에게도 무한한 감사의 마음 전합니다. 동시에 동료들에게 몇마디 감히 전해 드리고 싶습니다. 아마도 지금 학위과정을 거치고 있는 많은

동료들이 학문과 그 외적 요소들 사이의 어쩔 수 없는 간극으로 인해 힘들어 하고 있을 것으로 생각합니다. 저 또한 같은 나이대의 주위 친구들이 먼저 사회에 나가 여러 모습들로 성공하고 부를 축적하는 모습을 지켜보면서 흔들린 적이 없지 아니하였던 것은 아닙니다. 뿐만 아니라 제도적으로 과학분야가 아주 풍요로운 지원을 받지는 못하는 터라 각자가 하고싶은 연구를 맘껏 할 수 없다는 데에서 오는 어려움 또한 분명 있을 겁니다. 하지만 다들 굳센 마음으로 견디고 버티고 지혜롭게 이겨내시길 바랍니다. 여러분이 겪는 어려움들은 여러분의 잘못으로 인한게 아니기에 너무 자책하지 마시고 헛웃음 몇 번으로 훌훌 털고 다시 연구에 매진하실 수 있기를 바랍니다. 오늘보다 나은 내일 그보다 더 찬란한 당신의 앞날이 있을 거라고 저는 믿어 의심치 않습니다. 여러분 또한 스스로를 믿으시기 바랍니다. 그리고 학문으로 오는 고통이 너무 괴로울 땐 잠시 스스로에게 기운 차릴 시간을 주는 그런 여유를 조금은 부리셔도 괜찮을 것 같습니다. 너무 과하게는 말구요. 이게 제가 소중한 여러분께 드리고 싶은 주제넘은 조언이자 응원입니다.

여러분들과 함께 했던 지난 10 년의 기억들은 앞으로도 제 인생에 있어 머릿속에 그리고 마음속에 가장 큰 자리를 차지할 것입니다. 감사드립니다. 엘에이엠알 화이팅!

2019 년 1 월 어느날

연구실 한편에서

김 종 인